UC-404
LBL-28688

Center for Advanced Materials

CAM

To be published as a chapter in **Structure of Electrified Interfaces**, J. Lipkowski and P.N. Ross, Eds., Vol. II, VCH Publishers, New York, NY, in process

Surface Crystallography at the Metal-Gas Interface

M.A. Van Hove

February 1990

For Reference

Not to be taken from this room

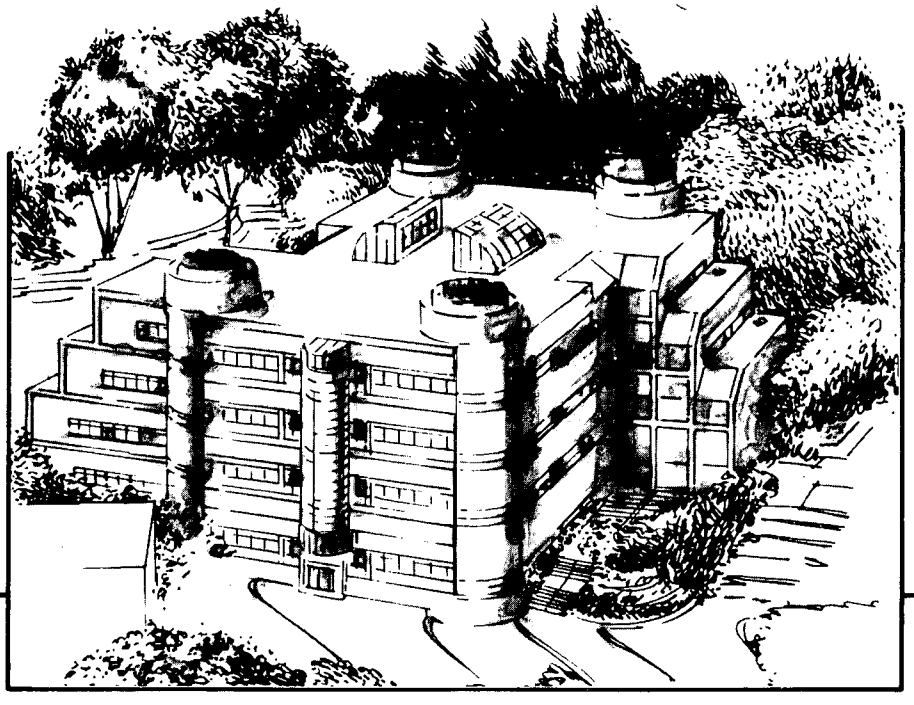

Materials and Chemical Sciences Division

Lawrence Berkeley Laboratory • University of California

ONE CYCLOTRON ROAD, BERKELEY, CA 94720 • (415) 486-4755

Prepared for the U.S. Department of Energy under Contract DE-AC03-76SF00098

LBL-28688
Copy 1
Bldg. 50 Library.

DISCLAIMER

This document was prepared as an account of work sponsored by the United States Government. While this document is believed to contain correct information, neither the United States Government nor any agency thereof, nor the Regents of the University of California, nor any of their employees, makes any warranty, express or implied, or assumes any legal responsibility for the accuracy, completeness, or usefulness of any information, apparatus, product, or process disclosed, or represents that its use would not infringe privately owned rights. Reference herein to any specific commercial product, process, or service by its trade name, trademark, manufacturer, or otherwise, does not necessarily constitute or imply its endorsement, recommendation, or favoring by the United States Government or any agency thereof, or the Regents of the University of California. The views and opinions of authors expressed herein do not necessarily state or reflect those of the United States Government or any agency thereof or the Regents of the University of California.

LBL-28688

Chapter 1 on
Surface Crystallography at the Metal-Gas Interface
by M.A. Van Hove
for Vol. II on "Structure of Electrified Interfaces",
J. Lipkowski and P.N. Ross, eds.
in Series "Frontiers of Electrochemistry"

1. Surface Crystallography at the Metal-Gas Interface

M.A. Van Hove

Center for Advanced Materials,

Materials and Chemical Sciences Division,

Lawrence Berkeley Laboratory,

Berkeley, CA 94720, USA

This work was supported by the Director, Office of Energy Research, Office of Basic Energy Sciences, Materials Sciences Division of the U.S. Department of Energy under Contract No. DE-AC03-76SF00098.

Table of contents:

Abstract

1.1 Introduction

1.2 Methods of surface structure analysis

1.2.1 Sample preparation

1.2.2 Diffraction and interference methods

1.2.3 Scattering methods

1.2.4 Microscopic and topographic methods

1.2.5 Complementary methods

1.2.6 Theoretical methods

1.3 Two-dimensional ordering principles

1.4 Two-dimensional crystallographic nomenclature

1.5 Clean surfaces

1.5.1 Unreconstructed surfaces

1.5.2 Stepped surfaces

1.5.3 Surface reconstruction

1.5.4 Alloy surface structure

1.6 Adsorption on surfaces

1.6.1 Physisorption

1.6.2 Atomic chemisorption

1.6.3 Metallic adsorption

1.6.4 Molecular chemisorption

1.6.5 Coadsorption

1.7 Outlook

Acknowledgements

Abstract

Methods and results of surface structure determination of the metal-gas interface are reviewed. Experimental techniques that operate in ultra-high vacuum have produced a large database of surface crystallographic results. Of particular relevance to the metal-liquid interface are several effects that have been discovered at the metal-gas interface, such as: relaxation and reconstruction of clean surfaces, adsorbate-induced relaxations and reconstructions, surface segregation of alloys, coadsorbate-induced ordering, and molecular distortions upon chemisorption.

1.1 Introduction

The atomic-scale structure and properties of the metal-gas interface have been extensively investigated in the last two decades[1−4]. Thanks to the availability of ultra-high vacuum techniques, it has become possible to control the composition and condition of this interface at the atomic and molecular level, and to determine its structure by using electrons and other probes[3−6].

The metal-gas interface can serve as an atomistically-controlled model for the metal-liquid interface[7,8]. It enables the study of the bonding of atoms and molecules directly to the metal surface, before the influence of the liquid is introduced. Many of the properties of the metal-gas interface are thus expected to be highly relevant to the understanding of the metal-liquid interface.

Similarly, the metal-gas interface serves as a model for the understanding of many other phenomena, such as heterogeneous catalysis, oxidation and corrosion, friction and

wear. The results presented here will therefore also be applicable to those technologically-important disciplines.

For the purposes of this discussion, we shall define the metal-gas interface as a region of space limited to a few atomic diameters on either side of the interface plane. We shall treat both the clean surface, before adsorption of gases, and the adsorbate-covered surface. The substrate can be bimetallic, whether originating in an alloy or artificially structured by deposition of one metal onto another. The substrate is a single-crystal surface, but it can "reconstruct" into a surface lattice different from the bulk lattice.

One can identify several levels of detail in the description of structure on single-crystal surfaces, as observed experimentally. One level of detail is given typically by a diffraction pattern, provided by the commonly available technique of low-energy electron diffraction, which indicates the presence or absence of ordering on the surface. This often is sufficient to indicate whether atomic adsorbates order on the surface, or whether molecules lie flat on a surface, for example. A second level of detail identifies a surface specie: thus vibrational spectroscopies can often tell which molecular species result from the chemisorption of a gas-phase molecule, and sometimes their orientation with respect to the surface plane as well. A third level of detail defines the crystallographic bonding structure: here bond lengths and bond angles are the important quantities. We shall discuss all three levels of detail as appropriate, while generally emphasizing the more detailed bonding geometries.

In section 1.2 we shall describe the techniques used to study the metal-gas interface (as well as other solid-gas interfaces). Since many gases order into regular lattices when adsorbed on single-crystal surfaces, the causes of such ordering will be discussed in section

1.3, while notation for such ordering will be introduced in section 1.4. The structures of clean and adsorbate-covered surfaces will then be presented in sections 1.5 and 1.6, respectively. And finally, an outlook into future developments will be offered in section 1.7.

1.2 Methods of surface structure analysis

In the following, we give a brief overview of the experimental methods used to study the structure of the metal-gas interface. Some aspects of their theoretical underpinnings are included, because more or less complicated calculations are often required to extract geometrical information from the data. Only the main techniques will be discussed: many more are available, but have contributed less to our topic.

1.2.1 Sample preparation

Ultra-high vacuum in the 10^{-10} Torr range is a prerequisite for the atomic-scale control of a metal-gas interface. Such a vacuum allows a surface to remain in the same condition for hours, for the duration of the experiment[1].

Metal surfaces are commonly prepared from single-crystal rods by mechanical or spark cutting in air, thereby exposing a surface of selected crystallographic orientation. The sample is then introduced into the vacuum, where it can be cleaned of undesirable surface impurities, surface oxides, etc. (by ion bombardment, for instance) and finally smoothed by annealing.

Atoms and molecules are usually deposited from the gas phase in small amounts that generate controllable "coverages" on the surface, i.e. controllable surface densities in the range from a fraction of a monolayer to a few monolayers.

Atoms can be deposited on surfaces in different ways. One can adsorb molecules which decompose; if a heteroatomic molecule is used, e.g. H_2S to deposit S, then the undesired atoms are thermally desorbed. One can also create atoms by decomposing molecules well before they approach the surface, and direct these atoms at the surface. It is sometimes also possible to make impurity atoms diffuse from the bulk and segregate to the surface to achieve the same result.

Molecules are deposited as gases, often by increasing the pressure in the vacuum chamber by leaking in the desired gas. Sometimes microcapillary arrays are used to direct a stream of gas at the surface without increasing the overall chamber pressure markedly.

1.2.2 Diffraction and interference methods

The majority of known surface structures has been studied[9] with low-energy electron diffraction (LEED). Also important have been photoelectron diffraction and fine structure techniques. All of these techniques involve quantum wave interference of electrons.

LEED[10-12] uses as probes elastically diffracted electrons with energies in the 20-300eV range, which corresponds to electron wavelengths in the 0.5-2Å range. Mono-energetic electrons are beamed at a surface, from which they are diffracted. Only elastically scattered electrons are normally recorded. Inelastic scattering processes severely limit the penetration depth of such electrons into a surface to about 5-10Å. The diffraction pattern

is a convenient monitor of the surface condition. In particular, it tells about the long-range ordering of the surface, showing the two-dimensional periodicity parallel to the surface.

Interferences between different scattering paths also pick up the local surface structure information in the form of modulations of diffracted electron beam currents. Elastic interactions are strong enough that multiple scattering of electrons from one atom to another is important. This complicates the analysis of experimental diffraction data, but the necessary theoretical methods have been very successful in obtaining bond lengths and angles at surfaces of almost any chemical composition. The technique has recently been extended from ordered layers to the case of disordered layers of adsorbates on single-crystal substrates[13-15].

In photoelectron diffraction and the so-called fine structure techniques, electrons are excited locally in the surface by another incident probe and allowed to diffract from nearby atoms, thereby carrying structural information in modulations of the emitted electron current.

In the case of photoelectron diffraction[16], electrons are photoemitted from particular electronic orbitals, such as core levels in individual surface atoms. Often synchrotron radiation is used as a source of photons. Those electrons which have scattered from nearby atoms toward the detector interfere with electrons travelling directly from the emitting atom to the detector, in a way that depends on the local geometry. The electrons are emitted with kinetic energies in the 500-1000eV energy range, where single-scattering events dominate to give a qualitatively simple scattering picture (but multiple scattering must be taken into account for accuracy). The method has been applied primarily to the study of atomic chemisorption on single-crystal surfaces.

Particularly well known among the fine-structure techniques is surface extended x-ray absorption fine structure (SEXAFS)[17,18]. Again, photoelectrons are excited and allowed to scatter from nearby surface atoms. However, in this case the electrons return to the emitting atom and modulate (by wave interference) the emission process itself. This modulation is again interpreted in terms of the local geometry. Also, 1000eV is a typical electron kinetic energy, but here a single-scattering model is often adequate to interpret the experimental data. Any emitted particle can be chosen for detection, including photons, electrons and ions. Like photoelectron diffraction, this method has been applied primarily to the study of atomic adsorbates on single-crystal surfaces.

Related to the extended fine-structure techniques are the near-edge techniques, such as near-edge x-ray absorption fine structure (NEXAFS, also called XANES, for x-ray absorption near-edge structure)[19], NEXAFS is SEXAFS conducted at much lower electron kinetic energies, where multiple scattering is strong. This technique is nowadays primarily used to monitor excitations among valence electrons, from which structural information like molecular orientation and bond lengths is sometimes accessible.

Of great importance to surface crystallography is x-ray diffraction[20], with its inherent conceptual simplicity. However, long mean free paths of x-rays in metals permit the desired surface sensitivity only when grazing incidence and/or scattering are used (within a fraction of a degree from the surface plane). This requires extremely flat surfaces and strict control of diffraction angles, both challenging experimental conditions. Also a sufficient photon flux is required, often supplied by synchrotron radiation. X-ray diffraction has been used in first instance to study clean surface reconstructions. It is particularly suitable to investigate disordering phenomena, like surface roughness and surface phase transitions.

1.2.3 Scattering methods

A number of techniques rely on scattering, as opposed to interference, to obtain geometrical information from surfaces. Of particular value has been ion scattering at high energies (100-1000keV)[21]. Such ions (helium nuclei and protons are commonly used) are directed along bulk crystal axes at crystal surfaces. They can channel deep into the crystal between rows of atoms. But if surface atoms deviate from the ideal bulk lattice positions, the ions will scatter strongly back out of the surface from these non-aligned atoms. This conceptually simple approach has been used successfully for many clean and adatom-covered surfaces, as well as for buried solid-solid interfaces. Depending on the energy range used and other experimental choices, the technique is known under the names of medium-energy ion scattering (MEIS) or high-energy ion scattering (HEIS).

Another directionally-sensitive scattering technique is electron-stimulated desorption ion angular dependence (ESDIAD)[22]. Here electrons knock ions from the surface. The ions are found to travel in directions close to those of the broken bonds, providing direct information on molecular bond orientations (as well as vibrational amplitudes). This approach has been effective in particular with hydrogen-containing molecules such as NH_3 and H_2O (see also the article by C. Campbell in this volume).

Electrons with energies on the order of 500-2000eV are forward scattered by atoms, i.e. they are focussed in the forward direction as if by a converging electrostatic lens. Thus, photoelectrons and other secondary electrons generated at an atomic site in a surface produce peaks of emission in directions corresponding to bond directions in the surface. This property has been exploited to determine bond orientations at surfaces[16,23,24]. It has

been possible, for example, to determine the location of minority atoms in a bimetallic surface, or the site of interstitial atoms in a metallic surface, or also the orientation of CO molecules on metal surfaces.

1.2.4 Microscopic and topographic methods

A number of powerful techniques have been developed that study surfaces in a microscopic sense: they image directly individual microscopic parts of a surface rather than structure averaged over macroscopic distances. Some, like field-ion microscopy (FIM)[25,26,27] and scanning tunneling microscopy (STM)[28] image individual atoms. Near-atomic resolution can also be obtained with electron microscopy[29], which can image end-on individual rows of atoms. Other techniques, like scanning Auger microscopy (SAM)[30], low-energy electron microscopy (LEEM)[31] and photoelectron microscopy (PEM)[32,33], image larger regions with micron or submicron resolution. Often these techniques provide chemical specificity; for example, SAM can image one atomic element while ignoring all others.

1.2.5 Complementary methods

A number of other techniques have been extensively applied to study surfaces in a variety of useful ways[1]. A common well-established technique for the analysis of surface composition is Auger electron spectroscopy (AES). Several kinds of optical spectroscopy are available to study electronic excitations and surface vibrations. For the latter, infrared

spectroscopy (IR) has become particularly effective, and is of great value at the metal-liquid interface. Another vibrational spectroscopy uses electrons and is therefore limited to vacuum experiments: high-resolution electron energy loss spectroscopy (HREELS).

1.2.6 Theoretical methods

Theory has made great progress in modelling surfaces on the atomic scale, although much work is still needed to make the theoretical methods practical for all but the simplest surfaces[6,34–36]. Accurate results have been obtained for clean metal surfaces and atomic adsorbates thereon in terms of binding geometries and energies, as well as electronic structure and vibrational frequencies. Good results are also available for the smallest adsorbed molecules, such as carbon monoxide. However, larger molecules usually require more severe approximations in the calculations.

1.3 Two-dimensional ordering principles

A large number of ordered surface structures can be produced experimentally on single-crystal surfaces, especially with adsorbates[37]. As we shall describe in more detail below, ordering can manifest itself both as commensurate and as incommensurate structures. There are also many disordered surfaces. For selected surfaces, order-order and order-disorder phase transitions have been explored in considerable detail both experimentally and theoretically[3].

We shall define the surface coverage to be unity when each (1x1) substrate cell is occupied by one adsorbate. The term "monolayer" will indicate completion of a single

layer, after which the coverage can only be increased by starting a second monolayer lying on top of the first monolayer.

a) Adsorbate-adsorbate and adsorbate-substrate interactions.

The driving force for surface ordering originates, analogous to three-dimensional crystal formation, in the interactions between atoms, ions, or molecules in the surface region.

For adsorbates, an important distinction must be made between adsorbate-substrate and adsorbate-adsorbate interactions. The dominant adsorbate-substrate interaction is due to strong covalent or ionic chemical forces in the case of chemisorption, or to weak Van der Waals forces in the case of physisorption. Adsorbate-adsorbate interactions may be covalent bonding interactions, orbital-overlapping interactions, electrostatic interactions (e.g. dipole-dipole interactions), Van der Waals interactions, etc. These are many-body interactions that may be attractive or repulsive depending on the system.

In chemisorption it is usually the case that the adsorbate-adsorbate forces are weak compared to the adsorbate-substrate binding forces. The adsorbate-substrate interaction includes a corrugation parallel to the surface, favoring certain adsorption sites over others and implying barriers to diffusion. This imposes the constraint that only lattice sites be occupied. With weak adsorbate-adsorbate forces the locations of the adsorbed atoms or molecules are determined by the optimum adsorbate-substrate bonding.

The adsorbate-adsorbate interactions dominate the long-range ordering of any overlayer. In chemisorption, an adsorbate lattice is formed which is simply related to the substrate lattice. In the ordered case this yields commensurate superlattices, which repeat periodically across the substrate lattice. The most common of these are simple structures

with one adsorbate per superlattice unit cell. They occur for adsorbate coverages of 1/4, 1/3 or 1/2 per cell, for example.

An incommensurate relationship exists when there is no common periodicity between an overlayer and the substrate. Such a structure is dominated by adsorbate-adsorbate interactions rather than by adsorbate-substrate interactions. The classical example is that of rare-gas monolayers physisorbed (weakly adsorbed) on almost any substrate: the overlayer takes on a lattice constant that is unrelated to that of the substrate. Another example of incommensurate lattice formation occurs frequently when thin compound films are produced by exposure of an elemental substrate to a gas. Examples are metal oxides, nitrides, carbides and silicides. As soon as about one or two monolayers of the compound are formed on the surface, they frequently adopt their own lattice constant independent of the substrate lattice constant.

b) Effects of adsorbate coverage.

The surface coverage of an adsorbate is an important parameter in the ordering process. At low coverages, adsorbates may bunch together in two-dimensional islands: this can occur when there are short-range attractive adsorbate-adsorbate interactions. Within each island the interactions induce an ordered arrangement of adsorbates. Other adsorbates repel each other at close separations, and do not interact at the large separations: these are disordered at low coverages. But when their coverage is increased so that the mean interadsorbate distance decreases to about 3-5Å, the repulsive interactions induce and strongly influence ordering, favoring certain adsorbate configurations over others.

Most adsorbates (other than some metals) will not compress into an overlayer of unity coverage on the closest-packed metal substrates. Even when small adatoms like hydrogen

and oxygen are adsorbed on a dense metal surface, it is often difficult to increase the monolayer density to unity coverage, i.e. to occupy all equivalent sites. There appears to be a close-range repulsive force that keeps them apart by approximately a Van der Waals distance. One may attempt to compress the overlayer further by increasing the coverage, which is done by exposing the surface to the corresponding gas at high pressures. The result is either no further adsorption, or diffusion of the adsorbates into the substrate, forming compounds, or, if the temperature is low enough, formation of physisorbed multilayers.

c) Physical adsorption.

When adsorbates are physisorbed rather than chemisorbed (at suitably low temperatures), one also finds that the Van der Waals distance determines the densest overlayer packing. Here it is the Van der Waals force acting directly between the adsorbates that dominates. In this case, the optimum adsorbate-substrate bonding geometry can be overridden by the lateral adsorbate-adsorbate interactions, yielding for example incommensurate structures where the overlayer and the substrate have independent lattices. Thus, there are no unique binding sites in these systems. Furthermore, with physisorption a larger coverage is also possible through multilayer formation.

1.4 Two-dimensional crystallographic nomenclature

Single-crystal surfaces are characterized by a set of Miller indices that indicate the particular crystallographic orientation of the surface plane relative to the bulk lattice[3]. Thus, surfaces are labelled in the same way that atomic planes are labelled in x-ray crystallography. For example, a Pt(111) surface exposes a hexagonally close-packed layer of

atoms, given that platinum has a face-centered cubic bulk lattice. For reference, such a surface is often additionally labeled (1x1), thus Pt(111)-(1x1): this notation indicates that the surface is not reconstructed into a periodicity different from that expected from simple truncation of the bulk lattice. Figure 1 shows a number of clean unreconstructed low-Miller-index surfaces.

Most surfaces in fact exhibit a different periodicity than expected from the bulk lattice, as is most readily seen in the diffraction patterns of LEED: often additional diffraction features appear which are indicative of a "superlattice". This corresponds to the formation of a new two-dimensional lattice on the surface, usually with some simple relationship to the expected "ideal" (1x1) lattice. For instance, a layer of adsorbate atoms may occupy only every other equivalent adsorption site on the surface, in both surface dimensions. Such a lattice can be labelled (2x2): in both surface dimensions the repeat distance is doubled relative to the ideal substrate. In this example, the (1x1) unit cell of the surface is magnified by a factor 2.

This (2x2) notation needs to be generalized. First, it can take on the form (mxn), where the numbers m and n are two independent stretch factors in different surface directions. These numbers need not be integers. In addition, this new unit cell can be rotated by any angle about the surface normal: this is denoted as (mxn)R$\alpha°$, where α is the rotation angle in degrees, as originally proposed by Wood[38]. Thus, the Wood notation allows the (1x1) unit cell to be stretched and rotated; however, it conserves the angle between the two unit cell vectors in the plane of the surface, disallowing "sheared" unit cells.

A more general notation is available for all unit cells, including those that are sheared, so that the superlattice unit cell can take on any shape, size and orientation. It is the matrix

notation, defined as follows[3]. We connect the unit cell vectors $\mathbf{a}'$ and $\mathbf{b}'$ of the superlattice to the unit cell vectors $\mathbf{a}$ and $\mathbf{b}$ of the substrate by the general relations:

$$\mathbf{a}' = m_{11}\mathbf{a} + m_{12}\mathbf{b},$$

$$\mathbf{b}' = m_{21}\mathbf{a} + m_{22}\mathbf{b}.$$

The coefficients m_{11}, m_{12}, m_{21}, and m_{22} define the matrix

$$M = \begin{pmatrix} m_{11} & m_{12} \\ m_{21} & m_{22} \end{pmatrix}$$

which serves to denote the superlattice. The (1x1) substrate lattice and the (2x2) superlattice are then denoted by the matrices

$$\begin{pmatrix} 1 & 0 \\ 0 & 1 \end{pmatrix}$$

and

$$\begin{pmatrix} 2 & 0 \\ 0 & 2 \end{pmatrix}$$

respectively.

In LEED experiments, the matrix M is determined by visual inspection of the diffraction pattern, thereby defining the periodicity of the surface structure.

A superlattice is termed commensurate when all matrix elements m_{ij} are integers. If at least one matrix element m_{ij} is an irrational number, then the superlattice is termed

incommensurate. Superlattices can be incommensurate in one surface dimension or in both surface dimensions.

A superlattice can be caused by adsorbates adopting a different periodicity than the substrate surface, or also by a reconstruction of the clean surface. In Figure 2 several superlattices that are commonly detected on low-Miller-index surfaces are shown with their Wood notation.

High-Miller-index (stepped) surfaces

The atomic structures of high-Miller-index surfaces are composed of terraces, separated by steps, which may have kinks in them. Examples are shown in Figure 3. For example, the (775) surface of an fcc crystal consists of (111) terraces, six atoms wide, separated by steps of (111) orientation and single-atom height.

The step notation[39] compacts this type of information into the general form $w(h_t k_t l_t) \times (h_s k_s l_s)$. Here $(h_t k_t l_t)$ and $(h_s k_s l_s)$ are the Miller indices of the terrace plane and the step plane, respectively, while w is the number of atoms that are counted in the width of the terrace, including the step-edge atom and the in-step atom. Thus, the fcc(775) surface is denoted by 6(111) × (11-1), or also by 6(111) × (111) for simplicity.

1.5 Clean metal surfaces

Once a metal surface has been cleaned and annealed, it is frequently found that it has the two-dimensional periodicity which one would expect from simple ideal truncation of the bulk lattice parallel to the surface plane, implying the simple models shown in Figure 1. However, there a quite a few exceptions, called reconstructions. In the case of bimetallic

surfaces, there can additionally be surface segregation, i.e. the composition at the surface can differ from the bulk. In all cases, there is the further possibility that bond lengths and interlayer spacings near the surface can differ from the bulk.

1.5.1 Unreconstructed surfaces

Surface atoms have a highly asymmetrical environment: they have neighbors toward the bulk and in the surface plane, but none outside the surface. This anisotropic environment forces the atoms into new equilibrium positions. For clean unreconstructed surfaces, there is generally a contraction of bond lengths between atoms in the top layer and in the second layer under the surface, relative to the bond length in the bulk: the contraction is on the order of a few percent. This relaxation in the topmost interlayer spacing is larger the more open (or rougher) is the surface, i.e. the fewer neighbors the surface atom has[40]. Figure 1 illustrates this relaxation. The closest packed surfaces, such as fcc(111) and fcc(100), show almost no relaxation; there may even be a very slight expansion for Pd and Pt(111). Large inward relaxations occur by contrast at surfaces like fcc(110), with interlayer spacings contracted by about 10%. The contractions are material dependent, Pb(110) showing a particularly large interlayer spacing contraction of 16%[41].

Relaxations of interlayer spacings occur also deeper than the second layer, in a phenomenon called multilayer relaxation[40]. The amplitudes of multilayer relaxations decay approximately exponentially with depth. The deeper relaxations are by no means all contractions. Instead it is more common to have alternating contractions and expansions in the interlayer spacings.

1.5.2 Stepped surfaces

It is found that on well-annealed clean fcc and bcc metal surfaces, steps are of mono-atomic height, as shown in Figure 3. On hcp metal surfaces whose terraces have the basal-plane orientation (0001), steps are of double height. The difference is that on these hcp surfaces mono-atomic height steps alternate among two inequivalent structures and can compose a more favorable double-height step. Little is known about steps at bimetallic surfaces, but marked segregation effects can be expected.

At stepped and kinked surfaces the atoms at the edges are more exposed and are expected to exhibit large relaxations with the effect of causing a partial smoothing at these rough surface sites. There is little quantitative information documenting the magnitude of relaxation at these defect sites but the available experimental information (pertaining to surfaces with terraces of one or two atoms width) does suggest relaxations at the step edges that are comparable to those at open lower-Miller-index surfaces[40].

Relaxations parallel to the surface are also expected and observed for atoms at step edges[40]: they tend to relax sideways toward the upper terrace of which they are a part. The amplitude of the displacement is comparable to the relaxations observed perpendicular to rough surfaces. Such sideways relaxations can also propagate deeper below the surface, again with an exponential decay and an oscillatory character.

1.5.3 Surface reconstruction

The LEED patterns for certain clean surfaces deviate from the expected (1x1) pattern, i.e. indicate the presence of a superlattice due to reconstruction. These are due either to

atomic displacements away from their bulk lattice sites (displacive reconstruction) or to bond breaking and new bond formation, such that surface atoms are bonded to different atoms than the bulk structure would imply. Among the clean metal surfaces, nearly a dozen are known to reconstruct.

Various types of reconstruction occur, each being caused by a different mechanism. A mild form consists of rehybridization without bond breaking. An example is the displacive reconstruction of W and Mo(100), in which the metal atoms are displaced slightly to form zigzag strings of mutually bonded atoms parallel to the surface[42], as shown in Figure 4. A type of reconstruction that maintains bulk sites is exemplified by the missing-row structure of Ir, Pt, and Au(110)[43], illustrated in Figure 5: here half the surface atoms are "missing" from the ideal structure. In all these cases, some bond length relaxations like those in clean unreconstructed metal surfaces also take place.

Some reconstructions can be explained by the tendency for bond lengths to decrease as the bonding coordination decreases. A good illustration is presented by the reconstructions of the clean Ir, Pt and Au(100) surfaces[44], shown in Figure 6. In these three cases, the interatomic distance in the topmost layer shrinks by a few percent parallel to the surface. It then becomes more favorable for this layer to collapse into a nearly hexagonally close-packed layer rather than maintain the square lattice of the underlying layers.

1.5.4 Alloy surface structure

The clean surface alloys fall into two main categories: those for which the bulk alloy is ordered and those for which it is disordered.

It appears that the surface structures of ordered bulk alloys are generally also ordered and maintain the bulk concentration. NiAl and Ni_3Al in particular have been extensively studied and found to satisfy this principle[45,46]. For instance, Ni_3Al (as well as other Cu_3Au-type alloys) have a (100) face which exhibits the periodicity expected from the alternating bulk stacking of 50-50 mixed NiAl layers and of pure Ni layers, see Figure 7. Some bond length relaxations are also apparent. In the case of $Ni_3Al(100)$ they are consistent with the picture that the smaller Ni atoms sink into the surface deeper than the larger Al atoms do.

With disordered bulk alloys, the surface is most often also disordered, but surface segregation can be very marked and can be strongly layer-dependent, with the possibility of an oscillating layer-by-layer concentration. For instance, different crystallographic faces of the Pt_xNi_{1-x} alloy have been found to exhibit very different segregation behavior as well as a strong layer dependence[47].

Other alloys, exemplified by Cu-rich CuAl, are disordered in the bulk, but order at some faces for certain bulk compositions[48]. Thus the (111) face of αCu-16at%Al exhibits a $(\sqrt{3}\times\sqrt{3})R30°$ surface periodicity (relative to the (1x1) surface lattice of pure Cu(111)), as shown in Figure 8. The other low-Miller-index faces of this alloy do not order.

1.6 Adsorption on surfaces

A large number of atomic and molecular adsorbates have been studied on metal surfaces over the last two decades[37]. Very different structures are found when comparing physisorption with chemisorption, or when comparing atomic with molecular adsorption,

or when adding a second type of adsorbate. Such differences will be reviewed in this section.

1.6.1 Physisorption

At low enough temperatures most gas-phase species will physisorb on most surfaces. In many instances, the physisorbed state is short-lived (lifetime far below a second) and called a precursor state, because of a low barrier to a chemisorbed state. Little is known about the structure of these short-lived physisorbed species. With inert gases and with saturated hydrocarbons, however, physisorption is commonplace and stable on many types of substrate. These substrates include metals as well as inert surfaces such as the graphite basal plane. Over 60 such stable physisorbed structures have been reported in the form of LEED patterns.

The simpler among the observed LEED patterns for physisorbed species can often be easily interpreted in terms of structural models. The known Van der Waals sizes of the species lead to satisfactory structures which are more or less close-packed. This is especially straightforward with inert gases. Thus, with Xe in an incommensurate overlayer on Ag(111), the Xe-Xe and Xe-Ag interatomic distances correspond closely to Van der Waals distances[49]. With molecules, the best structural models usually involve flat-lying species, which are arranged in a close-packed superlattice. The flat geometry provides the greatest attractive Van der Waals interaction with the substrate. This has been established, for instance, by LEED for a sequence of saturated straight-chain hydrocarbons of varying length physisorbed on Pt(111)[50], cf. Figure 9.

1.6.2 Atomic chemisorption

Thousands of atomic chemisorption systems have been studied over the years[37]. It is very frequent that chemisorbed atoms order well on surfaces, particularly at specific coverages like 1/4, 1/3 or 1/2 per cell. In some cases, order-disorder transitions are observed as the temperature is raised (this requires that the transition temperature be lower than the temperatures where desorption into the vacuum or diffusion into the substrate start).

Adatoms often form simple overlayers with minimal effect on the substrate. But adatoms can also change the substrate structure, through relaxations or reconstructions or compound formation, etc. In the following, several of these structural aspects of atomic adsorption will be reviewed.

a) Adsorption sites

The simple atomic adsorption structures on metal surfaces are characterized by the occupancy of high-coordination sites[3,6,9], illustrated in Figure 10. Thus, Na, S, and Cl overwhelmingly adsorb over "hollows" of the metal surface, bonding to as many metal atoms as possible. The situation is slightly more complicated with the smaller adsorbates, H, C, N, and O. Although high coordination is still preferred, the small size of these atoms often allows penetration within or even below the first metal layer. The penetration is generally interstitial in metals. In any case the surface can reconstruct as a result, especially at higher coverages. For instance, a monolayer of N penetrates into interstitial octahedral sites between the first two layers of Ti(0001) with minimal distortion of the Ti lattice[51], cf. Figure 10f. Both C and N burrow themselves within the hollow sites of the Ni(100) surfaces so as to be almost coplanar with the topmost Ni atoms[52,53].

b) Bond lengths

The observed bond lengths between adatoms and substrate atoms generally fall well within 0.1Å of comparable bond lengths measured in bulk compounds and molecules[3,54]. In a few cases the accuracy is sufficient to detect significant variations in bond lengths. For example, when the surface coverage of cesium atoms is varied from 1/3 to 2/3 per cell on Ag(111), the Ag-Cs bond length is found to change from 3.20Å to 3.50Å[55]. This illustrates an expected effect of mutual interactions between adsorbates: the denser the adsorbate layer, the weaker the individual adatom-substrate bonds.

c) Adatom induced relaxations

When atoms adsorb on an inward relaxed clean surface and form chemical bonds, the inward relaxation is generally reduced, as the surface atoms of the substrate move back towards the ideal bulk-like positions or even beyond, as shown in Figure 10. Relaxations of deeper interlayer spacings are also much reduced upon adsorption[56].

Good examples of the outward relaxation of interlayer spacings are provided by atomic adsorption on the (110) surfaces of nickel and other fcc metals. The clean (110) surfaces typically exhibit contraction by about 10% (0.1 to 0.15Å) in the topmost interlayer spacing relative to the bulk value. Upon adsorption these contractions are reduced to less than 3 to 4% (0.03 to 0.05Å), often indistinguishable from the bulk value.

d) Adsorbate-induced surface restructuring

The adsorption of atoms may displace substrate atoms parallel to the surface to provide better adsorbate-substrate bonding. This is well illustrated by the effect of carbon adsorbed on Ni(100)[52], illustrated in Figure 11. The adatom buries itself into a four-fold

site, and pushes the neighboring nickel atoms sideways. The carbon atom thereby bonds also to a Ni atom in the second metal layer. The surrounding metal lattice cannot accept a corresponding compression at a coverage of 0.5 per cell and instead forces a rotation of the square of four Ni atoms about the surface normal. Thereby, the average metal density in the top layer is kept constant.

Oxygen in Ni(100) also induces substrate relaxations[57,58]. In the c(2x2) and p(2x2) structures, a buckling appears in the second Ni layer. The second-layer Ni atom directly below an oxygen atom (which is centered over a hollow site) is pulled up towards the oxygen atom, forming a partial bond.

The energy needed for surface restructuring is paid for by the increased bond energies between the adsorbed atom and the substrate. Therefore, such surface restructuring is expected only upon chemisorption where the adsorbate-substrate bond energies are similar to the bond energies between the atoms in the substrate. This is clearly the case for the adsorption of carbon, oxygen, and sulfur on many transition metals.

The chemisorption of atoms frequently removes a clean-surface reconstruction and produces a nearly bulk-like surface structure. Electron acceptors, like O and S, are particularly effective at removing clean-surface metal reconstructions.

Adsorbates have also been found to induce a number of new reconstructions. Even without being ordered, an adsorbate layer can induce a reconstruction. In some cases a small coverage (below 0.1 per cell) of disordered adsorbate can be sufficient to cause reconstruction of the substrate. Electron donors in particular, like alkali metals, are known to induce reconstructions. For instance, alkali adatoms Ni, Cu, Pd, and Ag(110) to the missing-row structure shown in Figure 5[59–62].

Reconstructions of stepped surfaces are frequently induced by the adsorption of O_2, H_2, etc. These restructuring phenomena can often be ascribed to the formation of a stable new phases like oxides, carbides and nitrides.

1.6.3 Metallic adsorption

More than 400 ordered surface structures of metal monolayers adsorbed on metal surfaces have been reported so far[37].

At low coverages, most of the metallic adsorbates form commensurate ordered overlayers: the overlayer unit cells are closely related to the substrate unit cells. Furthermore, in many cases a (1x1) LEED pattern is observed. This suggests that adsorbed metal atoms attract each other to form two-dimensional islands. The size of such islands can change depending on the substrate temperature, as can be detected by measuring the LEED spot size. A disordered LEED pattern is observed when the adsorbed metals repel each other. This is seen, for example, in the case of alkali metal adsorption on a transition metal[63], since the charged adatoms undergo repulsive interactions.

At higher coverages, the relative atomic sizes of the different metals becomes an important factor. When the atomic sizes of the substrate and adsorbate metals are similar, (1x1) structures are favored, which may include some stress due to the residual lattice mismatch[37]. On the other hand, coincidence structures often form when the atomic sizes are much different: here the substrate and overlayer lattices coincide at regular but larger intervals, as a compromise between the need to satisfy the adatom-adatom distances and the energetic advantage of commensuration with the substrate.

As the overlayer coverage increases towards a monolayer, the adsorbate-adsorbate interaction increases. Then an overlayer structure with out-of-phase domains is formed, reflecting the remaining strength of the substrate-adatom interaction. This is illustrated with the case of Pb adsorbed on Cu(100), cf. Fig. 12. The lead atoms form strips (domains) of c(2x2) structure, separated by domain walls of higher density. However, the closer-packed Pb atoms on either side of the domain walls repel each other into lower-symmetry sites than the preferred hollow site.

At higher coverages some metals can undergo layer-by-layer growth (Frank-Van der Merwe growth[64]), while other systems form three-dimensional crystallites (Volmer-Weber growth[65] into "balls"); still others fall between these two extremes and grow one monolayer followed by three-dimensional crystallites (Stranski-Krastanov growth[66]).

Alloy formation is frequently observed with suitable combination of adsorbate and substrate metals, usually at higher temperatures. However very few surface crystallographic data are available on such systems, and general trends cannot be drawn at this time.

1.6.4 Molecular chemisorption

Over 390 ordered LEED patterns have been reported for the adsorption of molecules. By far the most frequently studied substrates are metals. Platinum substrates have been most extensively used, due no doubt to their importance in both heterogeneous catalysis and electrochemistry. The most common adsorbates are CO, NO, C_2H_2 (acetylene),

C_2H_4 (ethylene), C_6H_6 (benzene), C_2H_6 (ethane), HCOOH (formic acid), and CH_3OH (methanol), reflecting the same technological applications.

Most molecular adsorption studies have been carried out near room temperature, with frequent cursory explorations of the higher-temperature behavior. Especially with molecules, temperature is a crucial variable, given the frequently diverse reaction mechanisms that can occur when molecules interact with surfaces. A number of studies have explored the lower temperatures, especially with the relatively reactive metal surfaces to the left of the Periodic Table, such as Fe, Mo, and W. At higher temperatures, decomposition of molecules is the rule. With hydrocarbons, sequential decomposition has been studied in greatest detail with the help of HREELS vibrational analysis[67].

The LEED patterns generally reflect disorder at high temperatures. Exceptions occur especially with carbon layers resulting from the decomposition of organic adsorbates: these may form either carbidic chemisorbed layers that are ordered or graphitic layers that have characteristic diffraction patterns[68].

Ordered LEED patterns for organic adsorption are frequent at lower temperatures. They can often be interpreted in terms of close-packed layers of molecules, consistent with known Van der Waals sizes and shapes. These ordered structures usually are commensurate with the substrate lattice, indicating chemisorption in preferred sites. It appears that many hydrocarbons lie flat on the surface, using unsaturated π-orbitals to bond to the surface. By contrast, non-hydrocarbon molecules form patterns that indicate a variety of bonding orientations. Thus CO is found to strongly prefer an upright orientation. However, upon heating, unsaturated hydrocarbon adsorbates evolve hydrogen and new species may be

formed which bond through the missing hydrogen positions. An example is ethylidyne, CCH_3, which can be formed from ethylene, C_2H_4, upon heating. Ethylidyne has the ethane conformation, but three hydrogens at one end are replaced by three substrate atoms. These issues will be discussed now in more detail.

a) Molecular adsorption sites and ordering

In discussing chemisorption geometries, it is useful to consider the bonding strength between a molecular specie and the metal surface on which it is adsorbed. When the bond is strong and localized, the molecule presents clear preferences for particular adsorption sites and it orders well. Thus, ethylidyne (CCH_3) bonds through one carbon atom to a three-fold coordinated hollow site on many fcc(111) surfaces, and typically orders as a (2x2) overlayer[69], see Figure 13.

When the molecular specie is large and bonds to many metal atoms simultaneously, as is the case with benzene lying flat on a surface, there is less preference for particular sites, which depend on the metal (and can easily be affected by coadsorbed species). Ordering is relatively weak under such conditions. In fact, benzene does not order at room temperature on Pd and Pt(111) surfaces, and only weakly on Rh(111).

In the case of weaker chemisorption, such as when CO or NO adsorb intact, there is also relatively little site preference and ordering is less pronounced as well: such molecules choose sites that depend on the metal and on the coverage, as well as on coadsorbates, while low order-disorder transition temperatures are found.

b) Carbon monoxide and nitric oxide adsorption

Detailed LEED studies of adsorbed CO and NO have been performed for a dozen surface structures, all on close-packed metal surfaces[70]. They have confirmed the site

assignments based on vibrational frequencies, as originally derived for metal-carbonyl and similar complexes. On many metals, CO prefers low-coordination sites at low coverages, e.g. linear coordination at top sites for CO on Ni and Cu(100), as shown in Figure 14. At higher coverages coordination generally increases, towards two-fold bridge sites and three-fold hollow sites (but apparently never four-fold hollow sites). The metal-C bond length has been found to increase with increasing coordination, as has the C-O bond length, again in agreement with metal-carbonyl complexes, confirming the C-O bond weakening implied by the decreasing vibration frequency.

At high coverages, crowding occurs and part of the CO and NO molecules have to settle for lower-symmetry sites. For instance, at a coverage of 3/4 per cell on Rh(111), one third of the adsorbed CO molecules occupy bridge sites, while the remainder are pushed off the top sites by about 0.4Å[71,72], as illustrated in Figure 15. NO in the same circumstances does the same thing, but the displacement from the top site is smaller, in accord with the smaller packing diameter of this molecule. There is no clear indication for CO tilting away from the surface normal in these structures, but tilting by up to 20° has been observed by LEED[73] and photoemission[74] in several other close-packed structures.

c) Straight-chain hydrocarbon adsorption

Acetylene and ethylene have been studied on several transition metal surfaces and are generally believed to lie flat on the surface when intact, based mainly on results from HREELS. Figure 16 shows this geometry for acetylene. Molecular distortions away from the linear or planar gas-phase configuration are expected from theory[75,76] and found with HREELS[77,78], while a lengthening of the C-C bond is observed experimentally with

NEXAFS[79]. These effects are due to strong rehybridization, as the carbons form strong new bonds to the metal atoms. The remaining C-C bonds are weakened, while C-C-H bond angles tend toward the tetrahedral angle.

The structure of methylacetylene has been analyzed with LEED[80]: it provides a close analogy with acetylene, with the added ability to show the distortion in the form of a methyl group rotation (LEED cannot easily tell hydrogen positions). The result confirms the flat arrangement derived for acetylene, cf. Figure 16. The triple C-C bond is found to indeed be considerably lengthened, to close to a single-bond length. And the third carbon atom (in the methyl group) is rotated by about 45° from the linear gas-phase configuration. This methyl group takes the place of one of the hydrogen atoms in Figure 16.

Ethylidyne can easily be produced from either acetylene or ethylene, by addition or subtraction of one hydrogen atom per molecule[69]. The C-C bond orients itself perpendicularly to the fcc(111) surface of several transition metals, cf. Figure 13. The bonding to the metal occurs at three-fold coordinated hollow sites. The resulting bond lengths are in close agreement with values found in organometallic complexes[81]. In particular, the C-C bond is intermediate in length between a single and a double bond. This adsorption structure is very stable against change of metal or coadsorption.

d) Benzene adsorption

Benzene adsorbs parallel to the fcc(100), fcc(111) and hcp(0001) surfaces, and probably on many other close-packed surfaces as well[82]. The adsorption site is variable, cf. Figure 17. On Pt(111), the molecule centers itself over a bridge site, whether benzene is mixed with CO or not. On Rh(111), the same site is found for a pure benzene layer, but

a three-fold hollow site emerges in the presence of coadsorbed CO. On Pd(111), in the presence of CO, the three-fold site is also found.

The height of the benzene carbon ring over the metal surface varies with the metal[82]: it is largest on Pd(111), smallest on Pt(111) and intermediate on Rh(111), taking the three surfaces for which this has been determined. Another, more remarkable, trend is an expansion of the carbon ring radius: the radius is close to the gas-phase value (1.40Å) on Pd(111), larger by about 0.35Å on Pt(111) and intermediate on Rh(111). These two trends indicate a metal-carbon bond strengthening and a carbon-carbon bond weakening when going from Pd to Rh and to Pt. Furthermore, there appears to be a reduction of the rotational ring symmetry from 6-fold, due to long and short C-C bonds: the symmetry is three-fold (with three mirror planes, as in the Kekulé distortion) when the adsorption site is a hollow of that symmetry, while it becomes two-fold (with two mirror planes) over a bridge site.

1.6.5 Coadsorption

Over 150 ordered surface structures have been formed upon coadsorption of two or more different atomic or molecular adsorbates[37]. In general, coadsorbed surface structures may be classified in two categories: cooperative adsorption and competitive adsorption. In cooperative adsorption, the two kinds of adsorbate mix well together and interpenetrate. In the competitive case the adsorbates segregate to form separate non-mixed domains. Generally, cooperative adsorption is found whenever the two species have opposite

donor/acceptor character, i.e. when one adsorbate is a donor while the other is an acceptor toward the metal substrate. Competitive adsorption occurs mostly when the two adsorbates are of similar type, i.e. both donors or both acceptors. Note, however, that some adsorbates, like CO, are somewhat ambivalent: the same adsorbate may sometimes be a donor and sometimes an acceptor.

For example, Na and S coadsorbed on Ni(100) mix and order well[83]. As a function of the two component coverages, different structures can be prepared, shown in Figure 18. But common to these structures is the fact that each adsorbate surrounds itself as much as possible with the other kind of adsorbate: so Na is surrounded by S and vice versa. This indicates an attractive interaction between a donor adsorbate and an acceptor adsorbate.

Coadsorption structures involving molecules have been extensively examined on Rh, Pt and Pd(111) using various pairs of adsorbates from the set C_2H_2, C_2H_3 (ethylidyne), C_6H_6, Na, CO, and NO[84]. Among these, the hydrocarbons and Na transfer electrons to Rh(111) when adsorbed: they are donors. CO and NO have the opposite electron-transfer character, and are therefore acceptors, at least in these cases.

The combination of ethylidyne and CO (or NO) on Rh(111), illustrated in Fig. 19, is particularly striking because it produces a molecular monolayer that is nearly chemically inert[85]: this monolayer can resist air at room pressure for minutes (instead of oxidizing instantaneously, as do most overlayer structures on metals). One must expect this layer to also chemically withstand the presence of most liquids at metal-liquid interfaces.

A further illustration of coadsorbate-induced ordering is the case of benzene mixed with CO on Pd, Rh and Pt(111)[82]. Benzene alone adsorbs in a disordered or weakly ordered

manner at room temperature. However, addition of CO to these disordered overlayers produces ordered surface structures, as shown in Fig. 20 for Rh(111).

Several mutual effects between coadsorbates have been seen. One effect is a site change. With CO, ethylidyne and benzene, site changes have been induced as a result of coadsorption[82,85]. For instance, pure ethylidyne on Rh(111) selects one of the two possible three-fold hollow sites (called hcp site); but after CO coadsorption, the ethylidyne site is changed to the fcc hollow site (which differs in the absence of a second-layer metal atom directly below the site). At the same time, CO is relocated by ethylidyne, from a top or bridge site to a hollow site(cf. Figure 19).

Another effect is a bond length change, which has been noticed in particular when another adsorbate is mixed into a CO layer[85]. Donor adsorbates induce a lengthening of the C-O bond by about 0.1Å (and frequently a site change towards higher coordination at the same time). Connected with this effect is a change in vibrational frequencies, again well illustrated with CO[84]: as the bond is lengthened, i.e. weakened, by coadsorption, the C-O stretch frequency decreases. These changes are generally also accompanied by charge transfers, as can be detected through work function changes.

1.7 Outlook

Surface crystallography at the metal-gas interface started about 20 years ago and has reached a stage where many simple structures have been solved in fair detail. The results have shown a number of important phenomena, such as: clean-metal relaxations

and reconstructions; surface segregation at the monolayer level in alloys; atomic adsorption at high-coordination sites with bond lengths close to those expected from known covalent radii; molecular species with geometries similar to those also found in analogous organometallic compounds; strongly stretched and/or distorted chemisorbed molecular species; coadsorbate-induced ordering and mutual distortions.

In more recent years, the phenomenon of adsorbate-induced restructuring has been observed with increasing frequency. Not only interlayer spacings within the substrate are changed by the adsorbate, but also lateral relaxations parallel to the surface and substrate layer bucklings are observed. This effect is likely to be more general than previously expected and many of the earlier structure determinations will have to be repeated with greater attention to such details.

The observation of coadsorbate-induced restructuring is an example of the increase in accuracy achieved in surface crystallography over the years. Another simultaneous improvement has been the ability to analyze increasingly complex and interesting structures. This has allowed the structure determination of complex surface reconstructions and coadsorbed molecular layers, for example.

Recently also, disordered overlayers have been made accessible to detailed local structure determination. It is safe to say that there are more disordered surface structures than ordered ones. Therefore, it is of great importance to extend this capability: one should expect a rapid increase in the investigation of such structures.

A new direction being developed at this time is that of stepped surfaces. Only a very limited class of stepped surfaces has been studied in any detail, namely clean surfaces

with narrow terraces (i.e. with not too high Miller indices). In view of the importance of steps as the primary type of surface defect where catalytic reactions can take place, it is imperative that adsorption structures at steps be investigated.

Non-metallic multilayers have hardly been investigated so far. Metallic and non-metallic multilayers are directly relevant to interfacial structures (e.g. grain boundaries), to mechanical bonding of different materials and epitaxial growth of one crystal on another. Much work lies ahead in this direction, as well.

Relatively few compound surfaces have been studied to date, whether prepared from bulk compounds or by formation of thin compound layers on pure substrates. Here also, numerous technologically interesting structures invite analysis.

Many of these new directions have direct relevance to the field of electrochemistry. The metal-liquid interface is drawing increasing attention on the part of investigators of the metal-gas interface. There is a strong effort to adapt the techniques which have been successful at the metal-gas interface to the case of the metal-liquid interface. Particularly notable are the efforts to apply x-ray diffraction and scanning tunneling microscopy to the metal-liquid interface.

Acknowledgement

This work was supported by the Director, Office of Energy Research, Office of Basic Energy Sciences, Materials Sciences Division of the U.S. Department of Energy under Contract No. DE-AC03-76SF00098.

References

1. G.A. Somorjai, "Chemistry in Two Dimensions", Cornell University Press (Ithaca, NY) 1981.
2. A. Zangwill, "Physics at Surfaces", Cambridge Univ. Press (Cambridge, UK) 1988.
3. M.A. Van Hove, W.H. Weinberg and C.-M. Chan, "Low-Energy Electron Diffraction: Experiment, Theory, and Structural Determination", Springer-Verlag (Heidelberg, Berlin) 1986.
4. M.A. Van Hove and S.Y. Tong, "Surface Crystallography by Low Energy Electron Diffraction: Theory, Computation and Structural Results", Springer-Verlag (Heidelberg, Berlin) 1979.
5. G. Ertl and J. Küppers, "Low Energy Electrons and Surface Chemistry", Verlag Chemie (Weinheim) 1985.
6. M.A. Van Hove, S.W. Wang, D.F. Ogletree and G.A. Somorjai, Adv. Quantum Chem. **20**, 1 (1989).
7. A.T. Hubbard, Chem. Rev. **88**, 633 (1988).
8. P.N. Ross and F.T. Wagner, in "Advances in Electrochemistry and Electrochemical Engineering", Vol. 13, p. 69 (1984).
9. J.M. MacLaren, J.B. Pendry, P.J. Rous, D.K. Saldin, G.A. Somorjai, M.A. Van Hove and D.D. Vvedensky, "Surface Crystallographic Information Service: A Handbook of Surface Structures", D. Reidel (Dordrecht, Holland) 1987; P.R. Watson, "Critical Compilation of Surface Structures Determined by LEED Crystallography", J. Phys. Chem. Ref. Data **16**, 953 (1987).

10. J.B. Pendry, "Low-Energy Electron Diffraction: The Theory and its Application to Determination of Surface Structure", Academic Press (London) 1974.

11. L.J. Clarke, "Surface Crystallography: An Introduction to Low-Energy Electron Diffraction", Wiley-Interscience (Chichester) 1985.

12. M.A. Van Hove, in "Chemistry and Physics of Solid Surfaces VII", Eds. R. Vanselow and R. Howe, Springer-Verlag (Heidelberg, Berlin) 1988, p. 513.

13. D.K. Saldin, J.B. Pendry, M.A. Van Hove, G.A. Somorjai, Phys. Rev. **B31**, 1216 (1985).

14. R.J. Rous, J.B. Pendry, D.K. Saldin, K. Heinz, K. Müller, and N. Bickel, Phys. Rev. Lett. **57**, 2951 (1986).

15. G.S. Blackman, M.-L. Xu, M.A. Van Hove and G.A. Somorjai, Phys. Rev. Lett. **61**, 2352 (1988).

16. C.S. Fadley, in "Synchrotron Research: Advances in Surface Science", Ed. R.Z. Bachrach, Plenum (New York) 1990, in press.

17. P.H. Citrin, J. Phys. (Paris), Colloque **C8**, 437 (1986).

18. J.E. Rowe, in "Synchrotron Research: Advances in Surface Science", Ed. R.Z. Bachrach, Plenum (New York) 1990, in press.

19. D.A. Outka and J. Stöhr, in "Chemistry and Physics of Solid Surfaces VII", Eds. R. Vanselow and R. Howe, Springer-Verlag (Heidelberg, Berlin) 1988, p. 201.

20. R. Feidenhans'l, Surf. Sci. Rep. **10**, 105 (1989).

21. J.F. van der Veen, Surf. Sci. Rep. **5**, 199 (1985).

22. T.E. Madey, in "The Structure of Surfaces", Eds. M.A. Van Hove and S.Y. Tong, Springer-Verlag (Heidelberg, Berlin) 1985, p. 264

23. W.F. Egelhoff, Jr., Crit. Rev. Solid State and Mat. Sciences, in press.

24. M.-L. Xu and M.A. Van Hove, Surf. Sci. **207**, 215 (1989).

25. E.W. Müller and T.T. Tsong, "Field Ion Microscopy", American Elsevier (New York) 1969.

26. G. Ehrlich, in "The Structure of Surfaces", Eds. M.A. Van Hove and S.Y. Tong, Springer-Verlag (Heidelberg, Berlin) 1985, p. 375.

27. T.T. Tsong and M. Ahmad, in "The Structure of Surfaces", Eds. M.A. Van Hove and S.Y. Tong, Springer-Verlag (Heidelberg, Berlin) 1985, p. 389.

28. Proc. 4th Int'l Conf. on STM/STS, J. Vac. Sci. Technol. **A8**, 153-726 (1990).

29. K. Takayanagi, J. Electron Microsc. **38**, Suppl., S58 (1989).

30. "Practical Surface Analysis: by Auger and X-ray Photo-electron Spectroscopy", Eds. D. Briggs and M.P. Seah, Wiley (Chichester, New York) 1983.

31. W. Telieps and E. Bauer, in "The Structure of Surfaces II", Eds. J.F. van der Veen and M.A. Van Hove, Springer-Verlag (Heidelberg, Berlin) 1988, p. 53.

32. M.E. Kordesch, W. Engel, G.J. Lapeyre, E. Zeitler and A.M. Bradshaw, Appl. Phys. A ??, ??? (1989), in press.

33. G.R. Harp and B.P. Tonner, Rev. Sci. Instrum. **59**, 853 (1988).

34. J. Sauer, Chem. Rev. **89**, 199 (1989).

35. S.G. Louie and M.L. Cohen, Ann. Rev. Phys. Chem. **35**, 537 (1984).

36. D.R. Hamann, in "Solvay Conference on Surface Science", Ed. F.W. de Wette, Springer-Verlag (Heidelberg, Berlin) 1988, p. 8.

37. H. Ohtani, C.-T. Kao, M.A. Van Hove, G.A. Somorjai, Progr. Surf. Sci. **23**, 155 (1987).

38. E.A. Wood, J. Appl. Phys. **35**, 1306 (1964).

39. B. Lang, R. W. Joyner, and G.A. Somorjai, Surf. Sci. **30**, 454 (1972).

40. F. Jona and P.M. Marcus, in "The Structure of Surfaces II", Eds. J.F. van der Veen and M.A. Van Hove, Springer-Verlag (Heidelberg, Berlin) 1988, p. 90.

41. J.W.M. Frenken, F. Huussen and J.F. van der Veen, Phys. Rev. Lett. **58**, 401 (1987).

42. D.A. King, Physics World **2**, 45 (1989).

43. E.C. Sowa, M.A. Van Hove and D.L. Adams, Surf. Sci. **199**, 174 (1988).

44. M.A. Van Hove, R.J. Koestner, P.C. Stair, J.P. Bibérian, L.L. Kesmodel, I. Bartoš and G.A. Somorjai, Surf. Sci. **103**, 189 and 218 (1981).

45. H.L. Davis and J.R. Noonan, in "The Structure of Surfaces II", Eds. J.F. van der Veen and M.A. Van Hove, Springer-Verlag (Heidelberg, Berlin) 1988, p. 152.

46. D. Sondericker, F. Jona, V.L. Moruzzi and P.M. Marcus, Sol. State Commun. **53**, 175 (1985).

47. Y. Gauthier, in "Physics of Solid Surfaces 1987", Ed. J. Koukal, Elsevier (Amsterdam) 1988, p.47.

48. R.J. Baird, D.F. Ogletree, M.A. Van Hove and G.A. Somorjai, Surf. Sci. **165**, 345 (1986).

49. N. Stoner, M.A. Van Hove, S.Y. Tong and M.B. Webb, Phys. Rev. Lett. **40**, 243 (1978).

50. L.E. Firment and G.A. Somorjai, J. Chem. Phys. **66**, 2901 (1977).

51. H.D. Shih, F. Jona, D.W. Jepsen and P.M. Marcus, Surf. Sci. **60**, 445 (1976).

52. J. Onuferko, D.P. Woodruff and B.W. Holland, Surf. Sci. **87**, 357 (1979).

53. L. Wenzel, J. Stöhr, D. Arvanitis and K. Baberschke, Phys. Rev. Lett. **60**, 2327 (1988).

54. K.A.R. Mitchell, S.A. Schlatter and R.N.S. Sodhi, Can. J. Chem. **64**, 1435 (1986).

55. G.M. Lamble, R.S. Brooks, D.A. King and D. Norman, Phys. Rev. Lett. **61**, 1112 (1988).

56. G.A. Somorjai and M.A. Van Hove, Progr. Surf. Sci. **30**, 201 (1989).

57. W. Oed, H. Lindner, U. Starke, K. Heinz, K. Müller and J.B. Pendry, to be published.

58. W. Oed, H. Lindner, K. Heinz, K. Müller, D.K. Saldin, P. de Andres and J.B. Pendry, to be published .

59. R.J. Behm, D.K. Flynn, K.D. Jamison, G. Ertl and P.A. Thiel, Phys. Rev. **B36**, 9267 (1987).

60. M. Copel, W.R. Graham, T. Gustafsson and S. Yalisove, Sol. St. Commun. **54**, 695 (1985).

61. C.J. Barnes, M.Q. Ding, M. Lindroos, R.D. Diehl and D.A. King, Surf. Sci. **162**, 59 (1985).

62. B.E. Hayden, K.C. Prince, P.J. Davie, G. Paolucci and A.M. Bradshaw, Sol. St. Commun. **48**, 325 (1983).

63. E.L. Garfunkel and G.A. Somorjai, Surf. Sci. **115**, 441 (1982).

64. F.C. Frank and J.H. Van der Merwe, Proc. Roy. Soc. **A198**, 205 (1949).

65. M. Volmer and A. Weber, Z. Phys. Chem. **119**, 277 (1926).

66. I.N. Stranski and L. Krastanov, Sitzungsker. Akad. Wiss. Wien. Math.-Naturwiss., Kl IIb, **146**, 797 (1938).

67. B.E. Bent, Ph.D. Thesis, University of California, Berkeley, (1986).

68. Z.P. Hu, D.F. Ogletree, M.A. Van Hove and G.A. Somorjai, Surf. Sci. **180**, 433 (1987).

69. R.J. Koestner, M.A. Van Hove, G.A. Somorjai, Surf. Sci. **121**, 321 (1982); J. Phys. Chem. **87**, 203(1983).

70. H. Ohtani, M.A. Van Hove and G.A. Somorjai, in "The Structure of Surfaces II", Eds. J.F. van der Veen and M.A. Van Hove, Springer-Verlag (Heidelberg, Berlin) 1988, p. 219.

71. M.A. Van Hove, R.J. Koestner, J.C. Frost and G.A. Somorjai, Surf. Sci. **129**, 482 (1983).

72. C.T. Kao, G.S. Blackman, M.A. Van Hove, G.A. Somorjai and C.-M. Chan, Surf. Sci., in press.

73. D.J. Hannaman and M.A. Passler, Surf. Sci. **203**, 449 (1988).

74. P. Hofmann, S.R. Bare, N.V. Richardson and D.A. King, Sol. St. Commun. **42**, 645 (1982).

75. A. Gavezzotti and M. Simonetta, Surf. Sci. **99**, 453 (1980).

76. D.B. Kang and A.B. Anderson, Surf. Sci. **155**, 639 (1985).

77. H. Ibach and S. Lehwald, J. Vac. Sci. Technol. **18**, 625 (1981).

78. H. Steininger, H. Ibach and S. Lehwald, Surf. Sci. **117**, 685 (1982).

79. J. Stöhr, F. Sette and A.L. Johnson, Phys. Rev. Lett. **53**, 1684 (1984).

80. M.A. Van Hove, C.-M. Chan, G. Casalone, R.J. Koestner and G.A. Somorjai, to be published.

81. M.R. Albert, J.T. Yates, Jr., "The Surface Scientist's Guide to Organometallic Chemistry", American Chemical Society (Washington, DC) 1987.

82. H. Ohtani, M.A. Van Hove and G.A. Somorjai, J. Phys. Chem. **92**, 3974 (1988).

83. S. Andersson and J.B. Pendry, J. Phys. **C9**, 2721 (1976).

84. C.M. Mate, B.E. Bent and G.A. Somorjai, J. Electr. Spectr. **39**, 205 (1986).

85. G.S. Blackman, C.T. Kao, B.E. Bent, C.M. Mate, M.A. Van Hove and G.A. Somorjai, Surf. Sci. **207**, 66 (1988).

Figure Captions

Fig. 1. Surface structures of low-Miller-index unreconstructed metal surfaces. In each panel a top view (above) and a side view (below) are shown. Dashed circles indicate ideal bulk positions of surface atoms, showing typically small relaxations perpendicular to the surface (drawn to scale).

Fig. 2. Commonly occurring superlattices on low-Miller-index metal surfaces, including their Wood notation.

Fig. 3. Atomic structures of flat and stepped surfaces of fcc metals. Shaded circles indicate step and kink atoms.

Fig. 4. Top view of the reconstructed W(100)-c(2x2) surface. Heavier circles represent top-layer W atoms displaced from a square array into zig-zag rows. Light circles show the second layer.

Fig. 5. Perspective view of fcc(110) surfaces, with the unreconstructed (1x1) termination at left and the (1x2) missing-row reconstruction at right. Arrows indicate atomic relaxations from ideal bulk positions. The largest arrow (not drawn to scale) represents a displacement of about 0.2Å.

Fig. 6. Reconstructions of Pt (top half) and Ir(100) (bottom half). Thin circles indicate second metal layer, with the ideal bulk square lattice. Thick circles correspond to top-layer atoms in a near-hexagonal lattice.

Fig. 7. Top view of $Ni_3Al(100)$, with mixed Ni/Al top layer and pure Ni second layer.

Fig. 8. Top view of the (111) surface of an ordered CuAl alloy, with a mixed Cu/Al top layer and a pure Cu second layer.

Fig. 9. Observed surface unit cells for n-paraffins on Pt(111). The dots indicate the Pt atomic positions. The five longer unit cells are believed to contain two molecules each.

Fig. 10. Top and side views (above and below in each panel) of common atomic adsorption geometries on various metal surfaces. Adatoms are shown as crosshatched circles. Dotted lines represent relaxed clean-surface atomic positions to illustrate adsorbate-induced relaxations (drawn to scale).

Fig. 11. Top view of a carbon structure on Ni(100). Carbon atoms are drawn as black filled circles. Each carbon atom is surrounded by a rotated square of 4 nickel atoms.

Fig. 12. Top view of a dense layer of Pb (drawn as large blank circles) on Cu(100). Three domain walls between c(2x2) strips are shown running up and down the page.

Fig. 13. Ordered structure of ethylidyne on an fcc(111) surface, in perspective view. The black bonds connect carbon atoms (very small circles) with hydrogen (medium-size circles) and metal atoms (large circles).

Fig. 14. Top view of carbon monoxide on Ni(100). CO molecules are shown end-on (with central perspective, giving appearance of non-parallelism), being perpendicular to the surface.

Fig. 15. Side view (above) and nearly perpendicular view (below) of a dense CO overlayer on Rh(111), indicating some interlayer spacings (full arrows) and bond lengths (broken arrows). Gray circles are C and O atoms; large open and black circles are first- and second-layer Rh atoms. Note how the CO overlayer is nearly hexagonal, thanks to deviations away from top sites.

Fig. 16. Perspective view of expected adsorption geometry of acetylene on several metal surfaces. Each carbon atom (medium-size circles) bonds to two metal atoms (large circles) and to a hydrogen atom (small circles), forming a non-linear molecule.

Fig. 17. Comparison of gas-phase benzene with benzene adsorbed in four structures on Pd, Rh and Pt(111), when mixed with CO (CO atoms are shown cross-hatched). Van der Waals radii are used to show the close packing in the molecular layer. Large dots indicate C nuclei, small dots second-layer metal atoms. Medium-size dots are guessed hydrogen positions. C-C distances are shown, while the average C-ring radius is listed below, together with the metal-C interlayer spacing and the frequency of the umbrella vibration mode of the hydrogen atoms.

Fig. 18. The coadsorption geometry of S (small shaded circles) and Na (large shaded circles) on Ni(100) (open circles), in top and side views (above and below): (a) coverages of 0.5 for both S and Na; (b) coverages of 0.5 and 0.25 for S and Na, resp.; (c) coverages of 0.25 for both S and Na.

Fig. 19. Side view (above) and nearly perpendicular top view (below) of a mixed CO + ethylidyne layer on Rh(111), showing selected interlayer spacings and bond lengths (hydrogen positions are guessed). Small and large circles represent CO and metal atoms, resp.

Fig. 20. Side and top views (above and below) of benzene coadsorbed with CO on Rh(111) in a 1:2 ratio, forming a (3x3) unit cell, which is outlined. Van der Waals radii are assumed for overlayer atoms. CO molecules are shaded. Large dots indicate C and O positions, medium dots indicate guessed hydrogen positions and small dots represent metal atoms in the second metal layer.

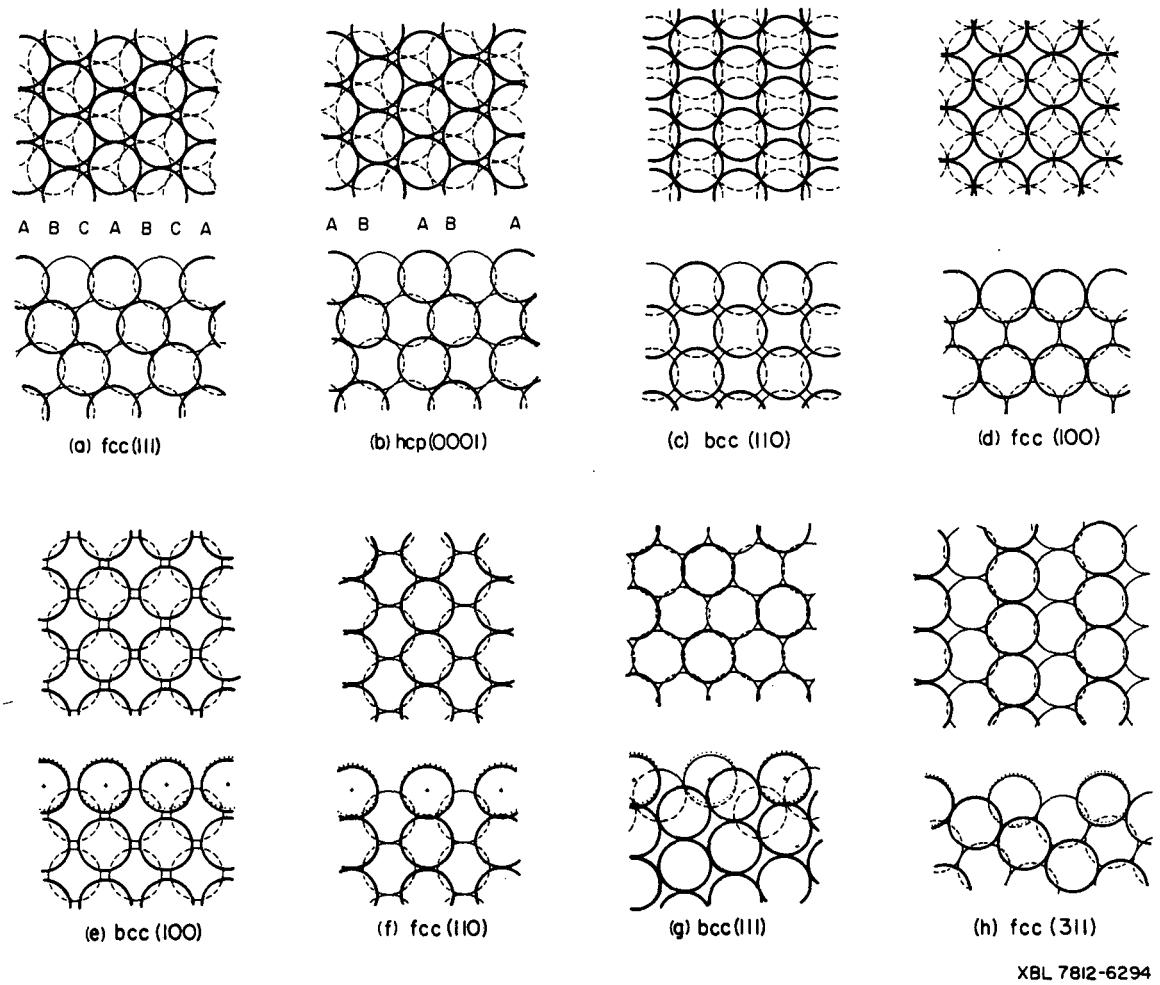
A B C A B C A
A B A B A
(a) fcc(111)
(b) hcp(0001)
(c) bcc (110)
(d) fcc (100)
(e) bcc (100)
(f) fcc (110)
(g) bcc(111)
(h) fcc (311)
XBL 7812-6294

Fig. 1

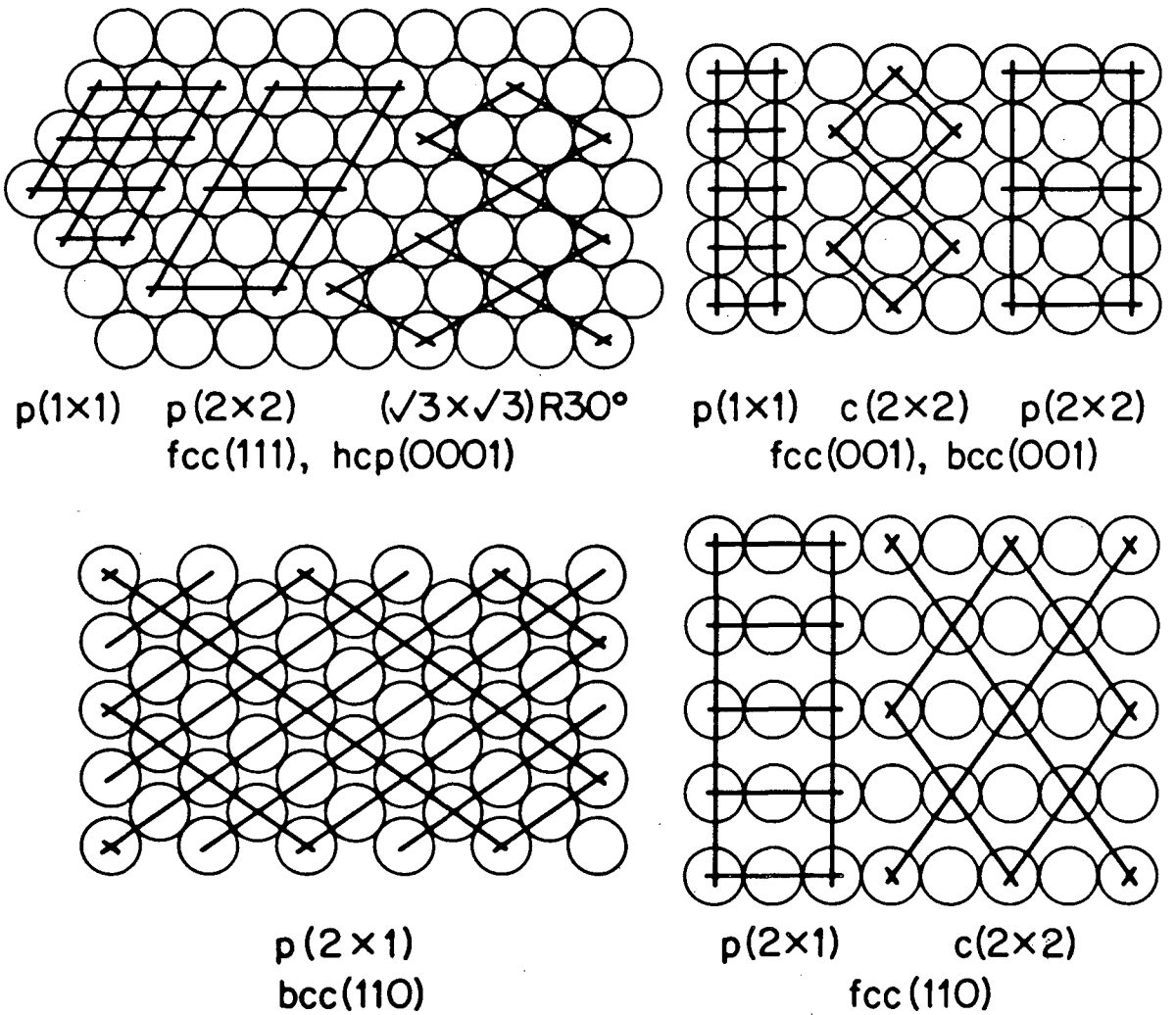

XBL 791-7763

Fig. 2

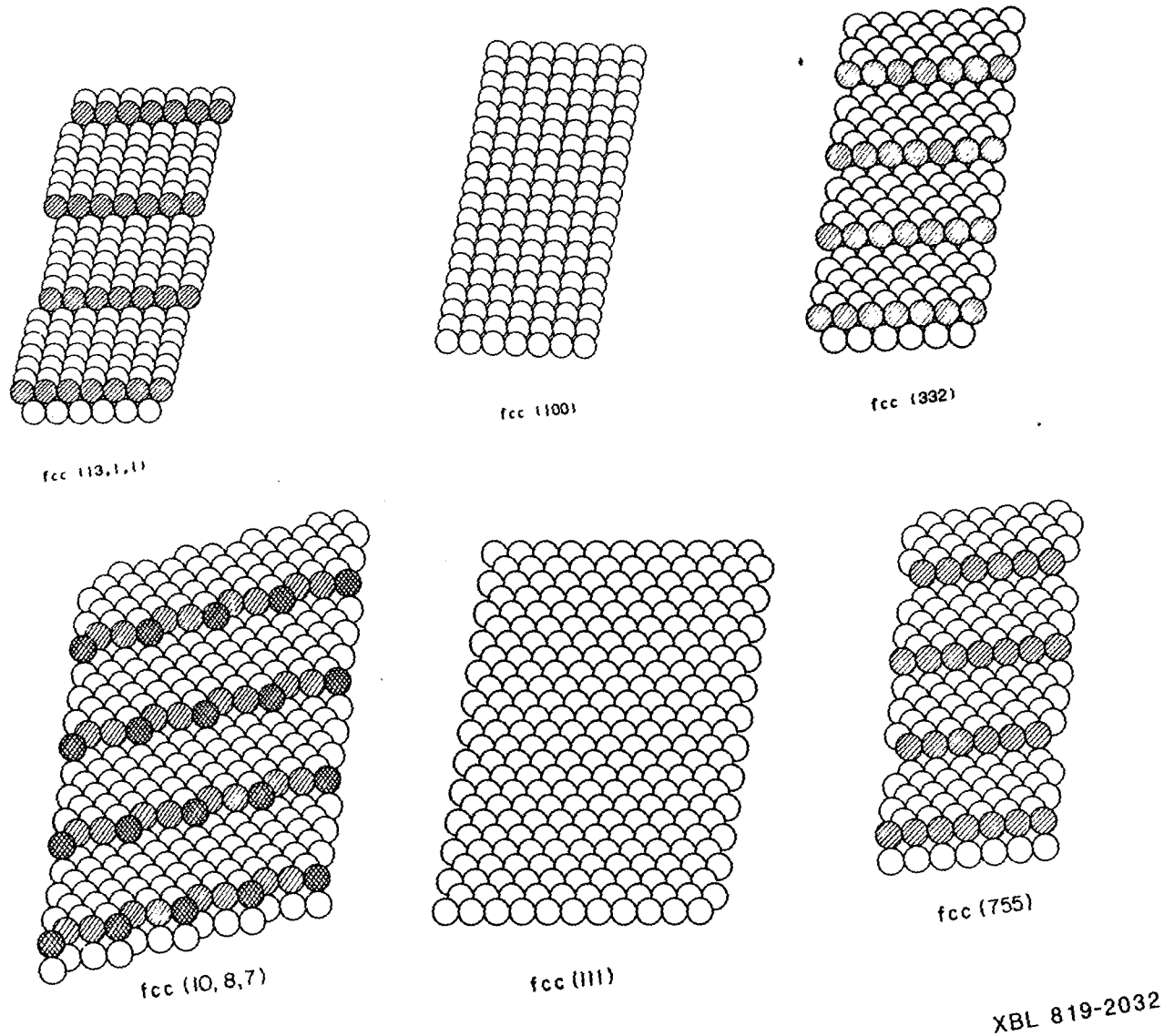

Fig. 3

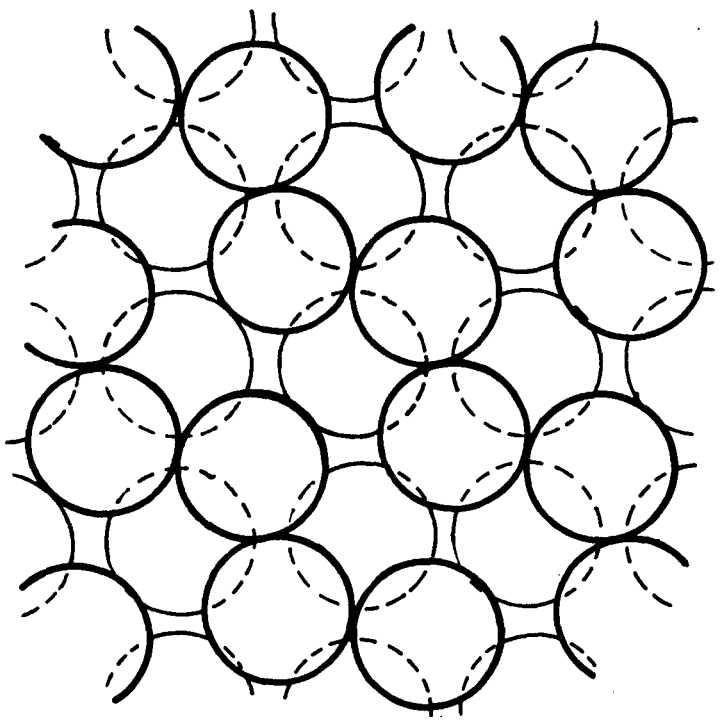

bcc (100) c(2x2)

XBL7812-6288

Fig. 4

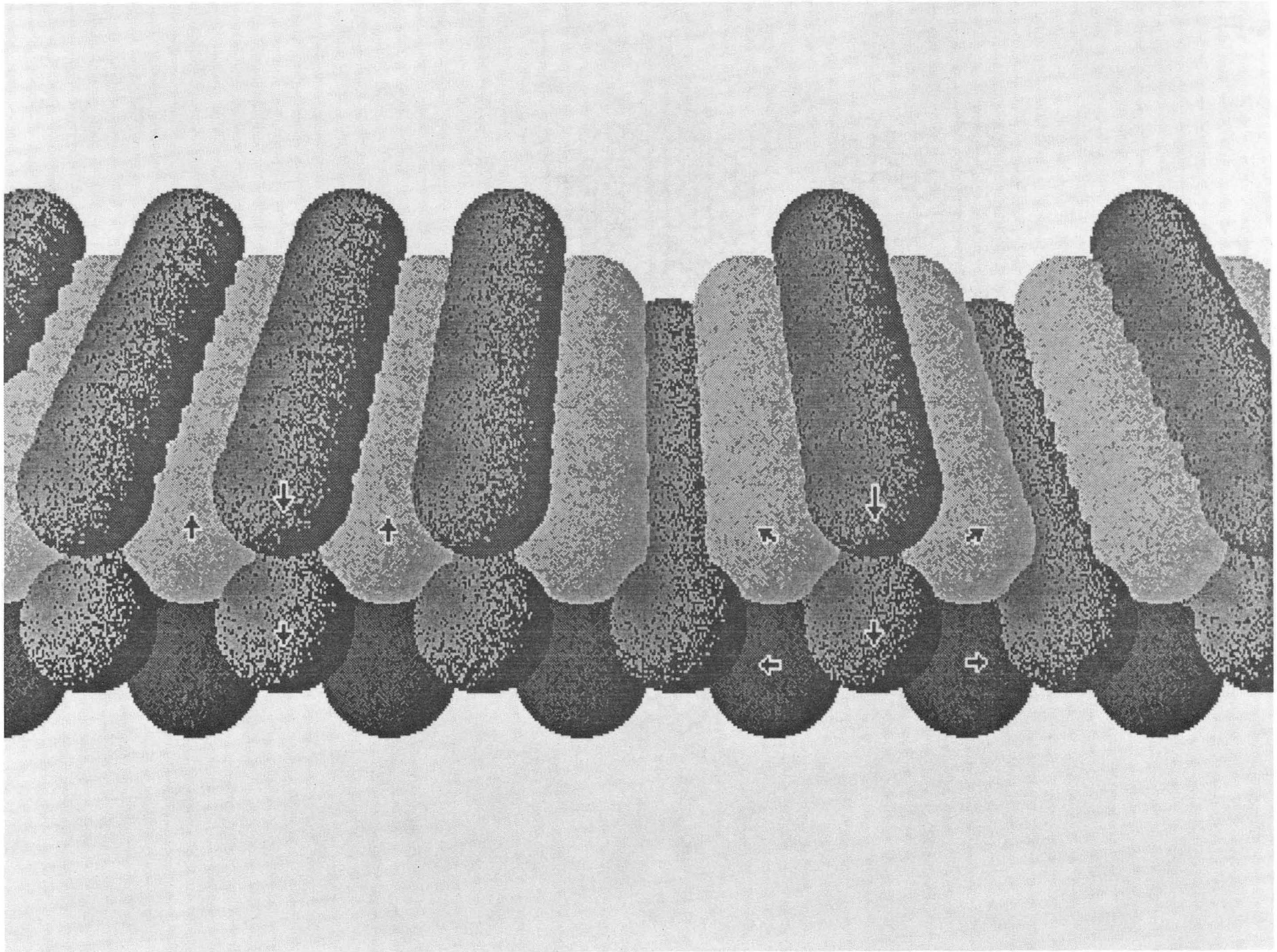

Fig. 5

XBB 895-3806

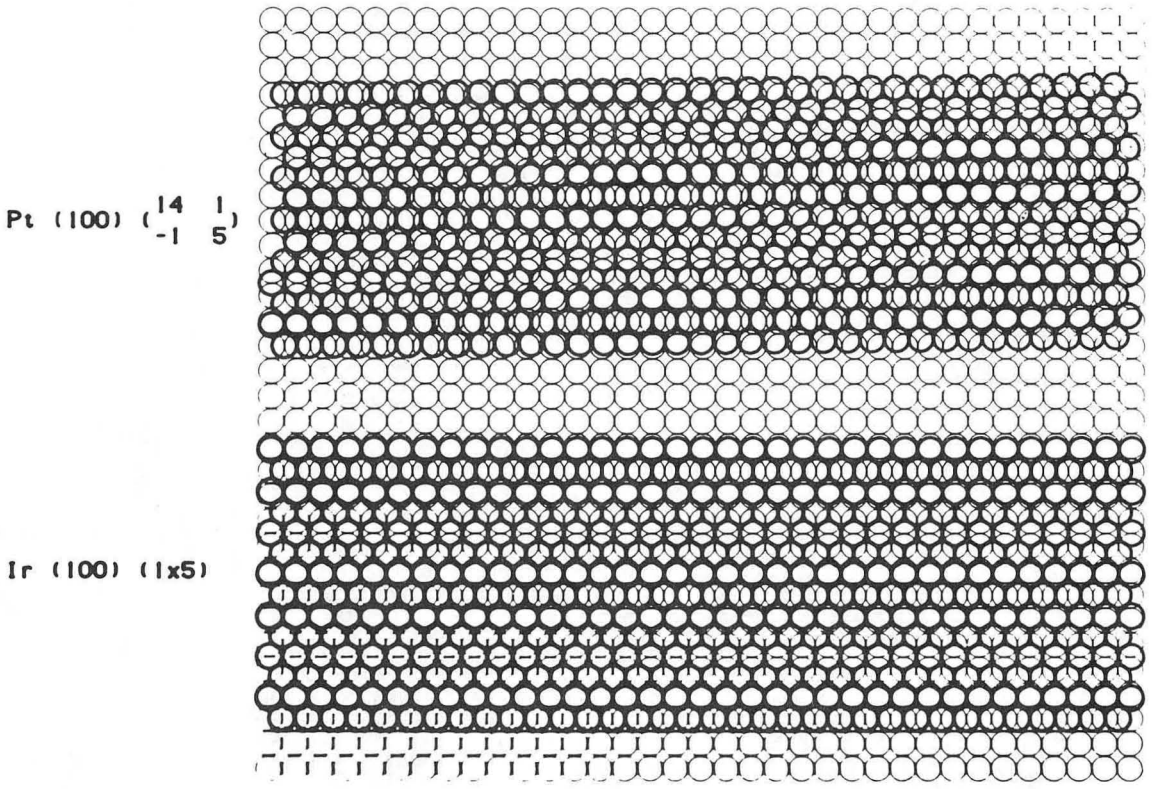

XBL 7912-13736

Fig. 6

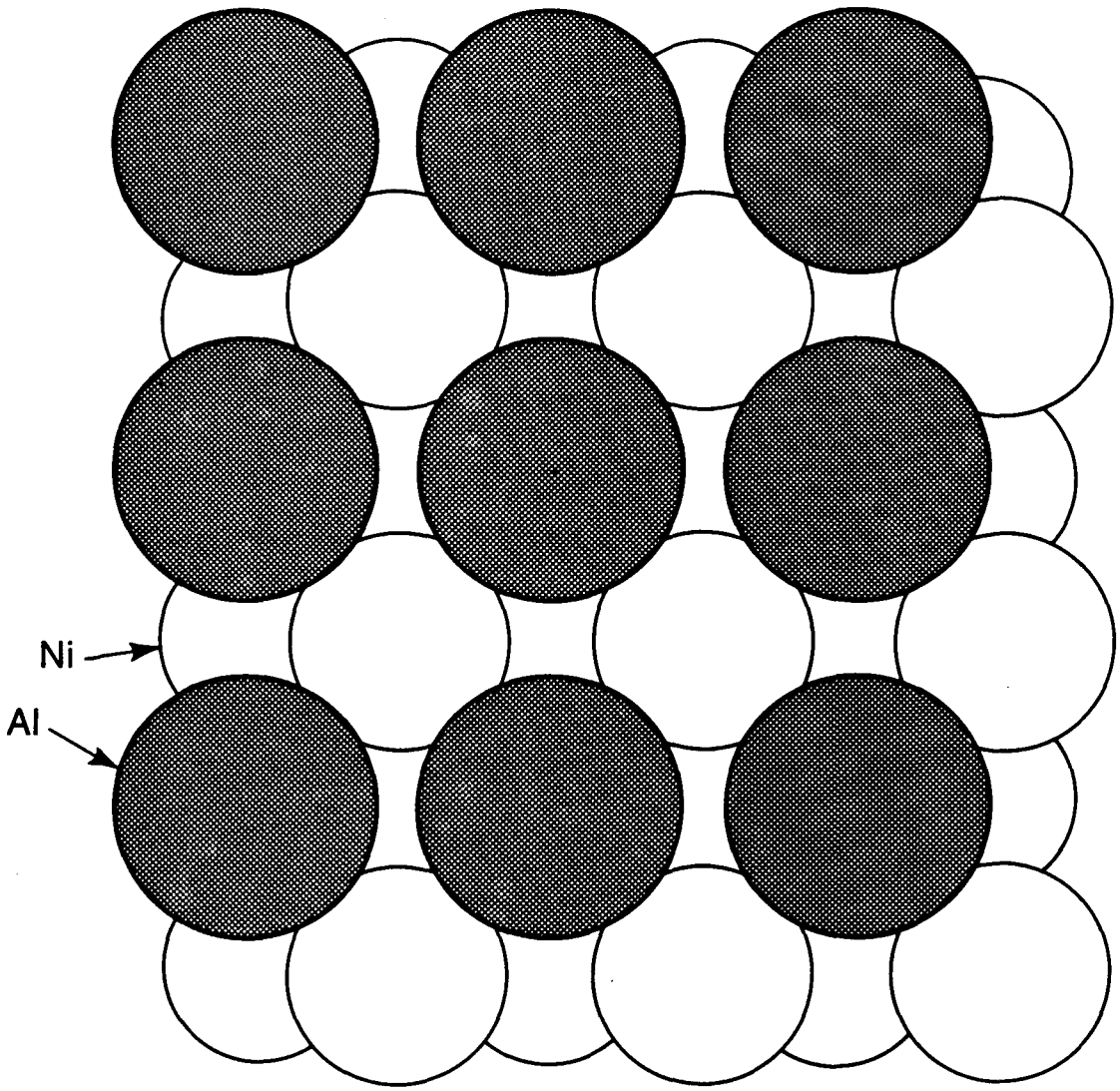

Ni_3Al (100) – (1 x 1)

XBL 8611-6523

Fig. 7

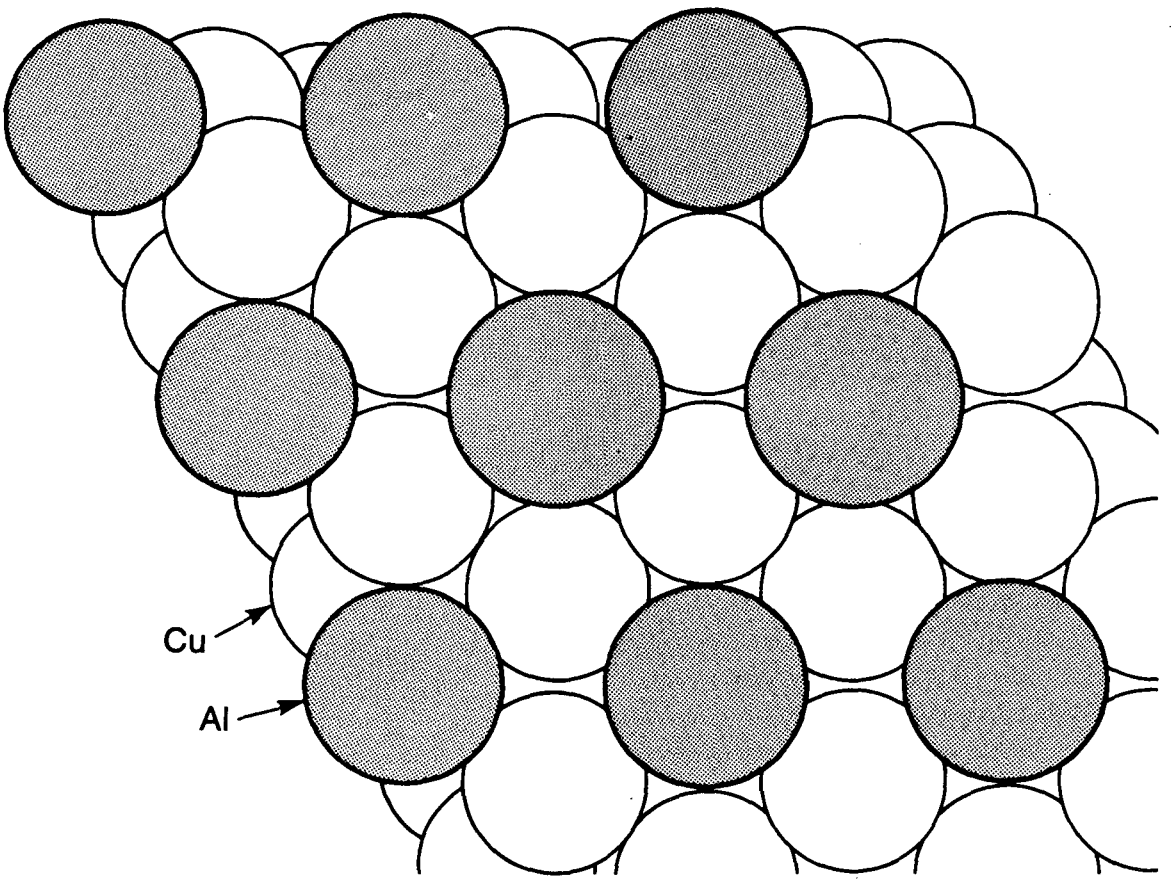

CuAl (111) – ($\sqrt{3}$ x $\sqrt{3}$) R30°

XBL 8611-6514

Fig. 8

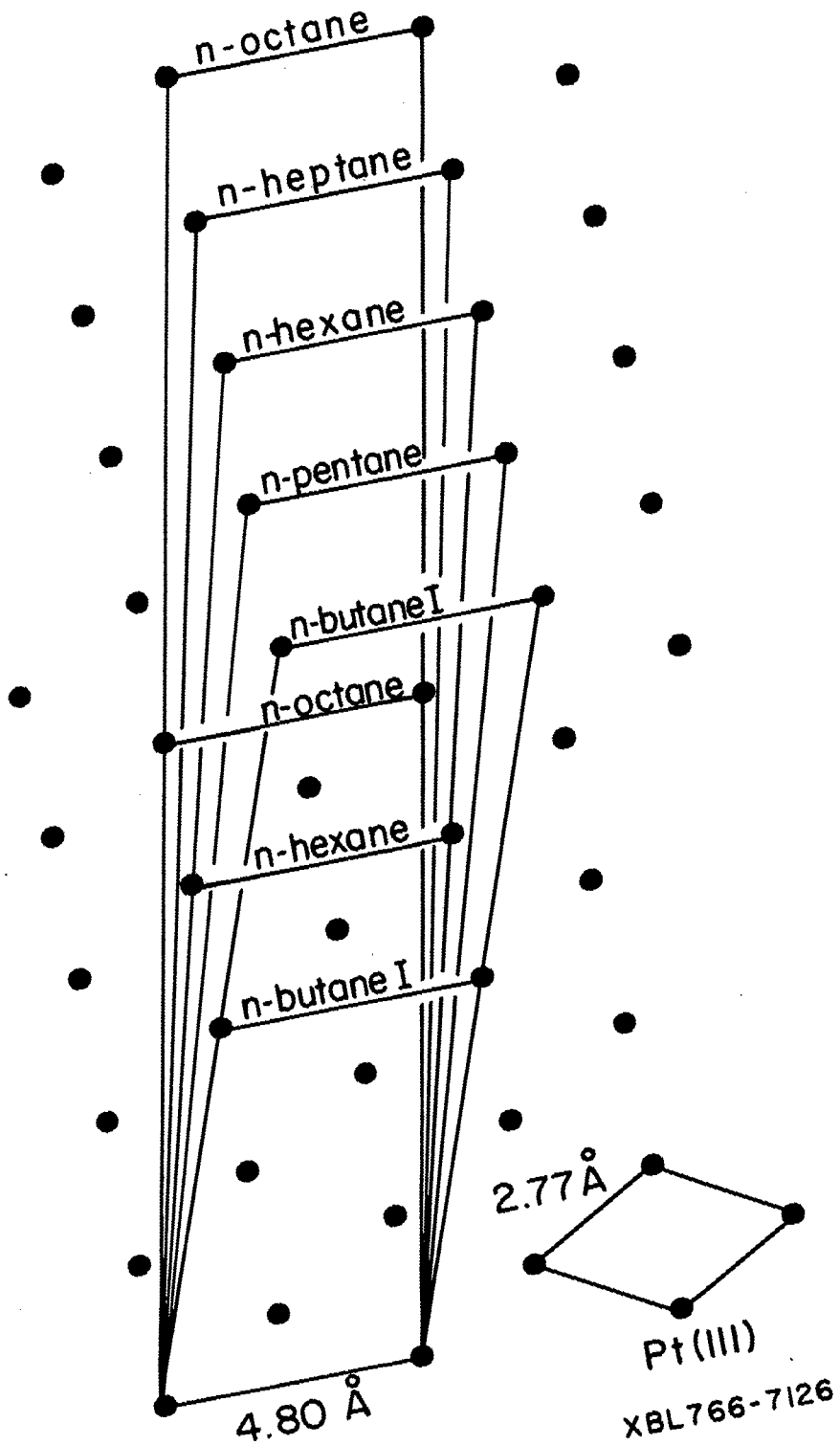
n-octane
n-heptane
n-hexane
n-pentane
n-butane I
n-octane
n-hexane
n-butane I
2.77 Å
Pt(111)
4.80 Å
XBL766-7126

Fig. 9

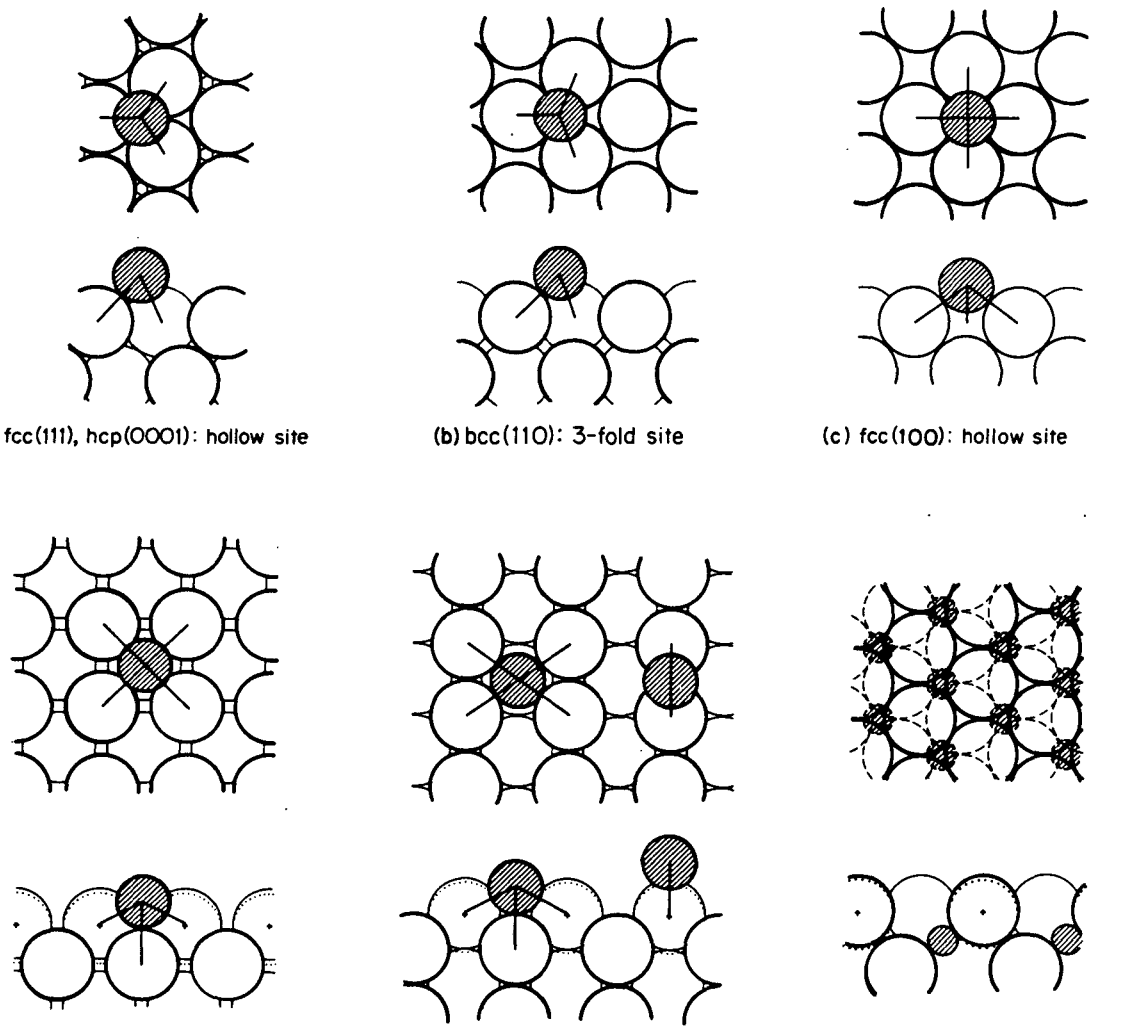

XBL 7812-6293

Fig. 10

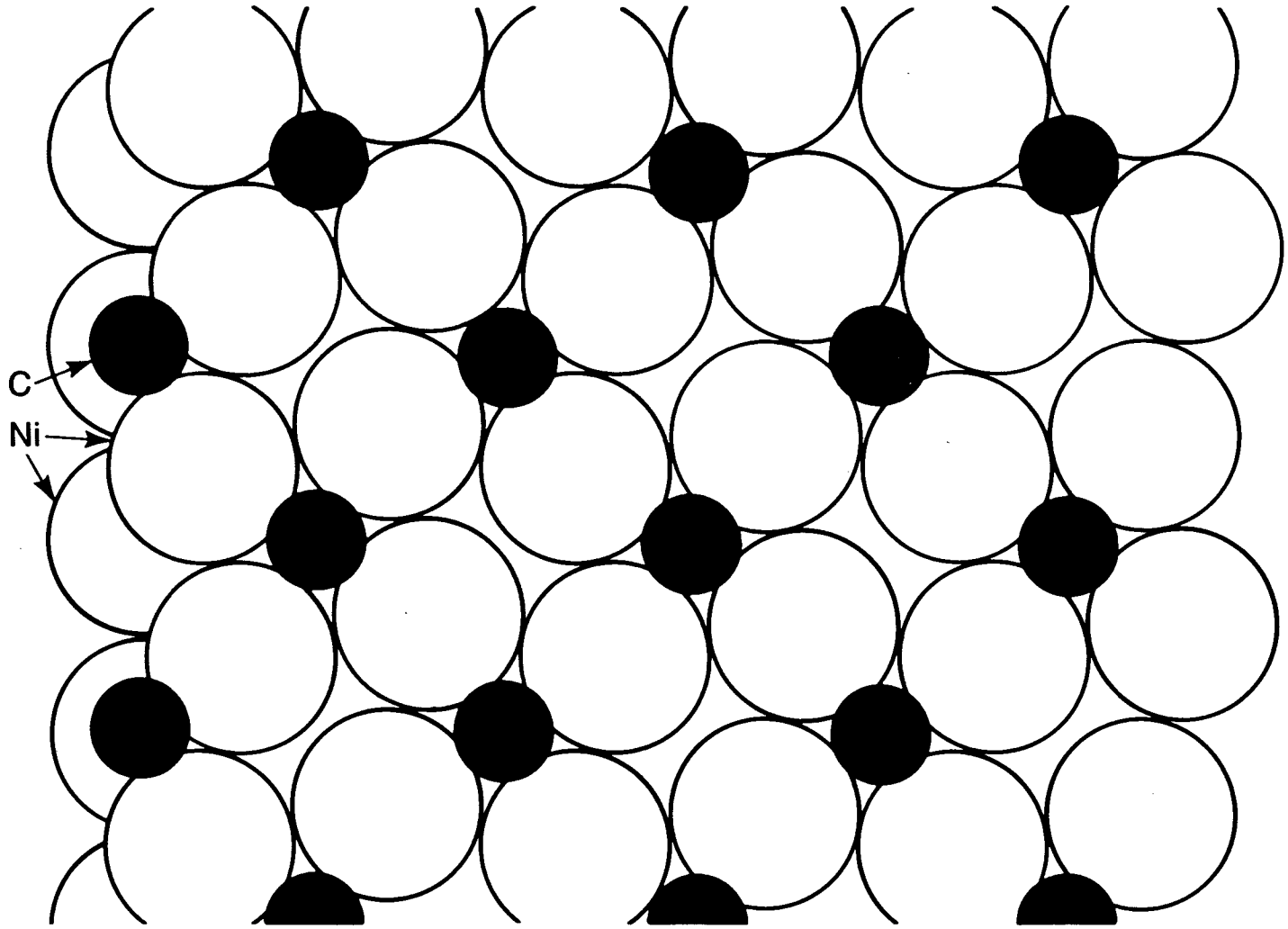

Ni (100) – (2 x 2) – 2C

XBL 8611-6513

Fig. 11

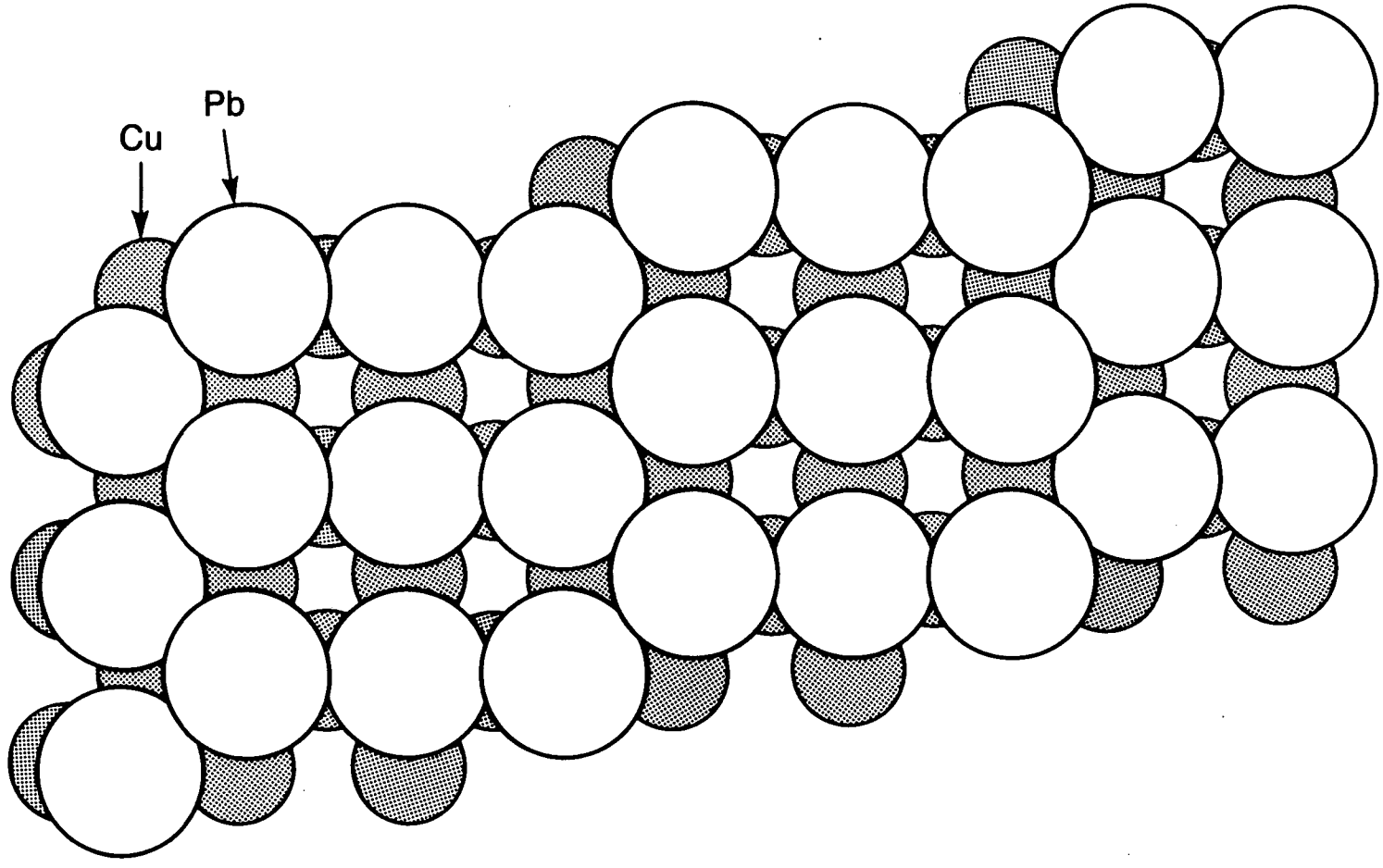

Cu (100) – c ($2\sqrt{2} \times \sqrt{2}$) R45° – 3Pb

XBL 8611-6520

Fig. 12

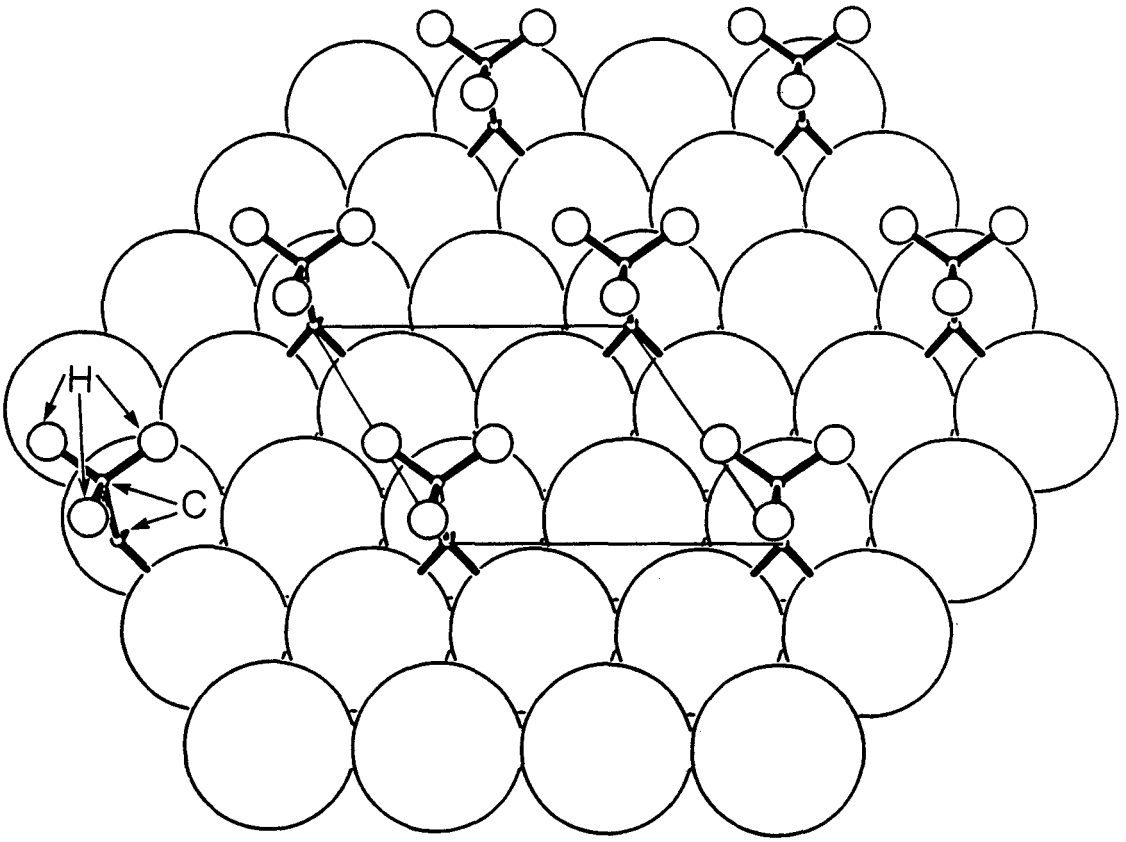

fcc (111) – (2 × 2) – C_2H_3 ethylidyne

XBL 871-9518

Fig. 13

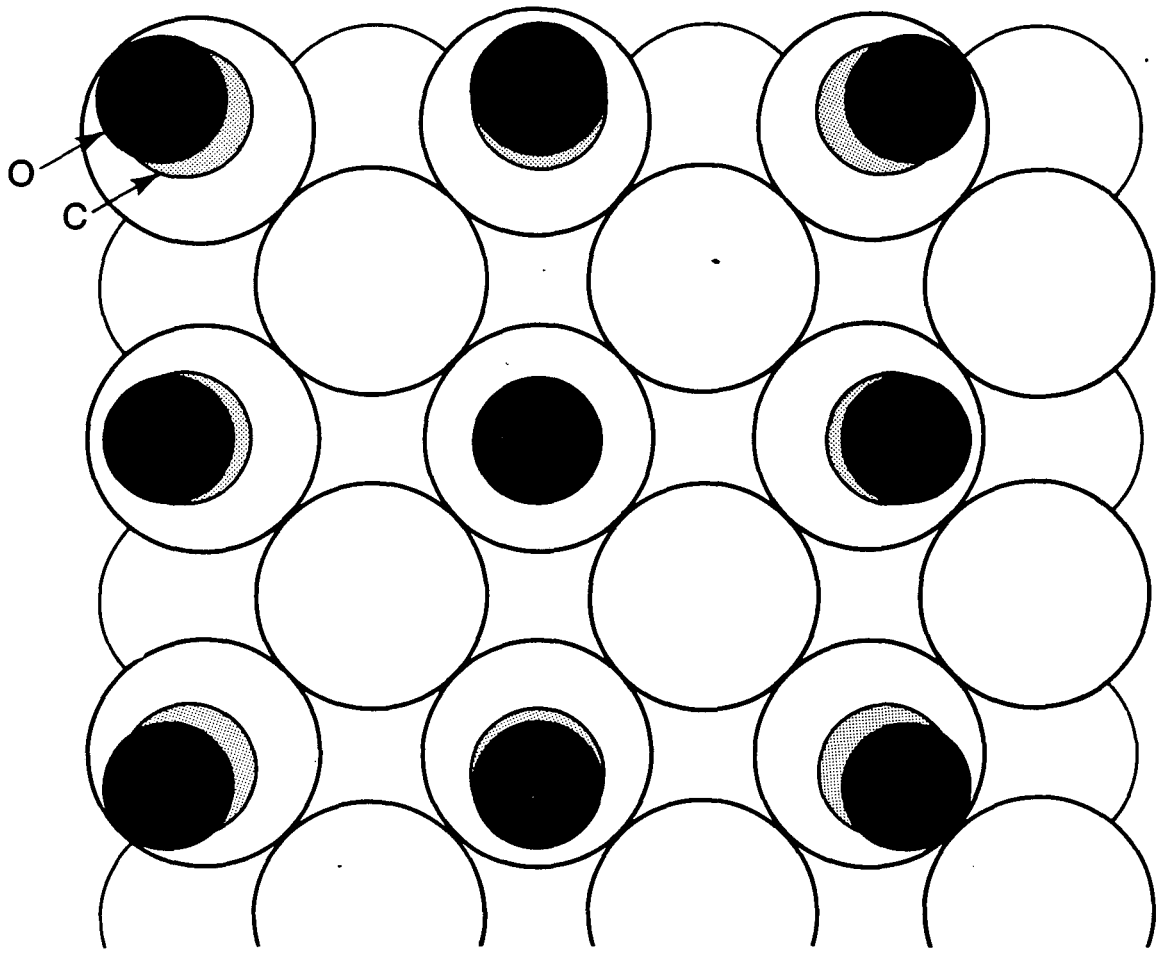

fcc (100) – c (2 x 2) – CO top sites

XBL 8611-6530

Fig. 14

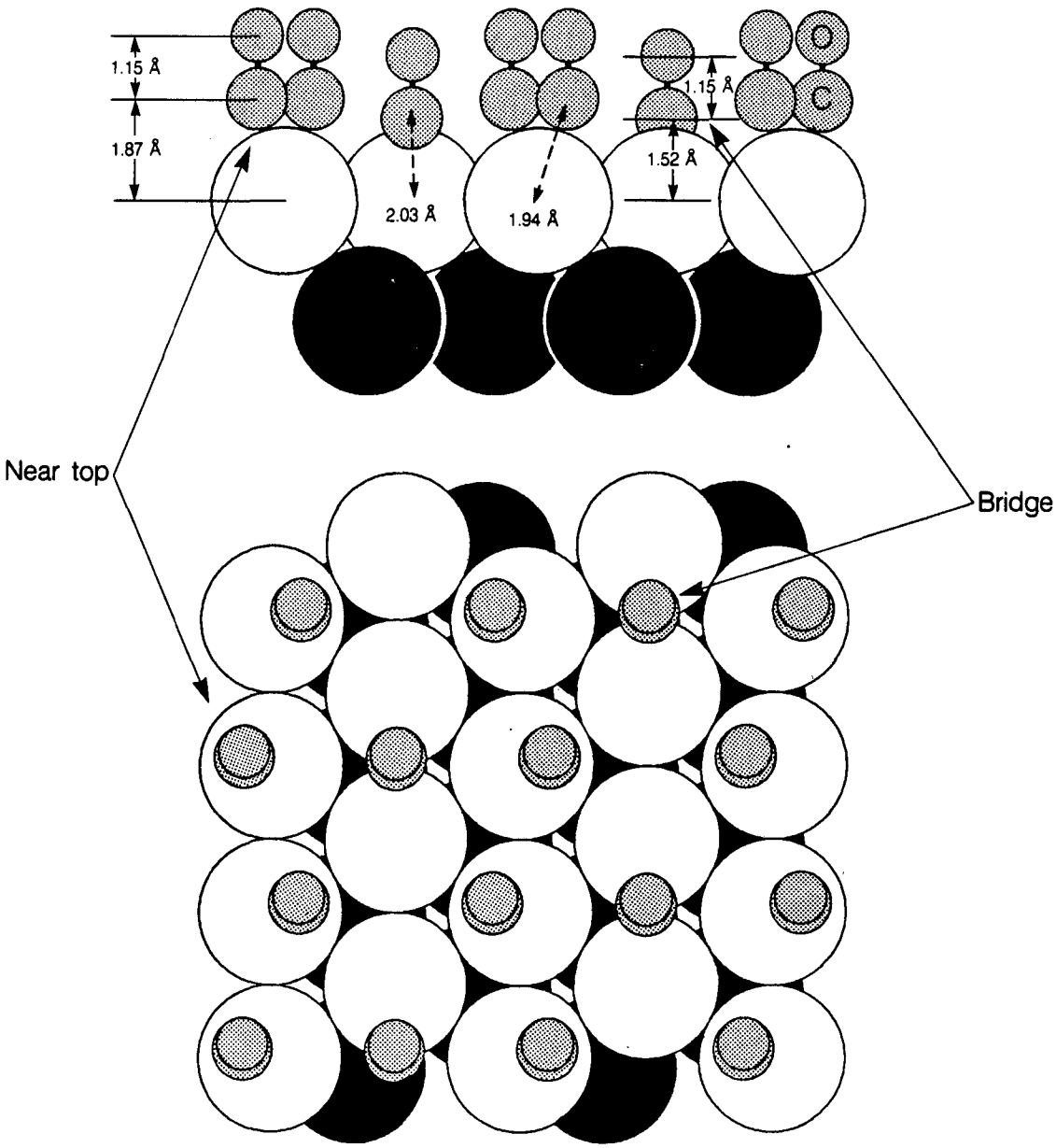

Rh(111) + (2X2) 3CO

XBL 895-6910

Fig. 15

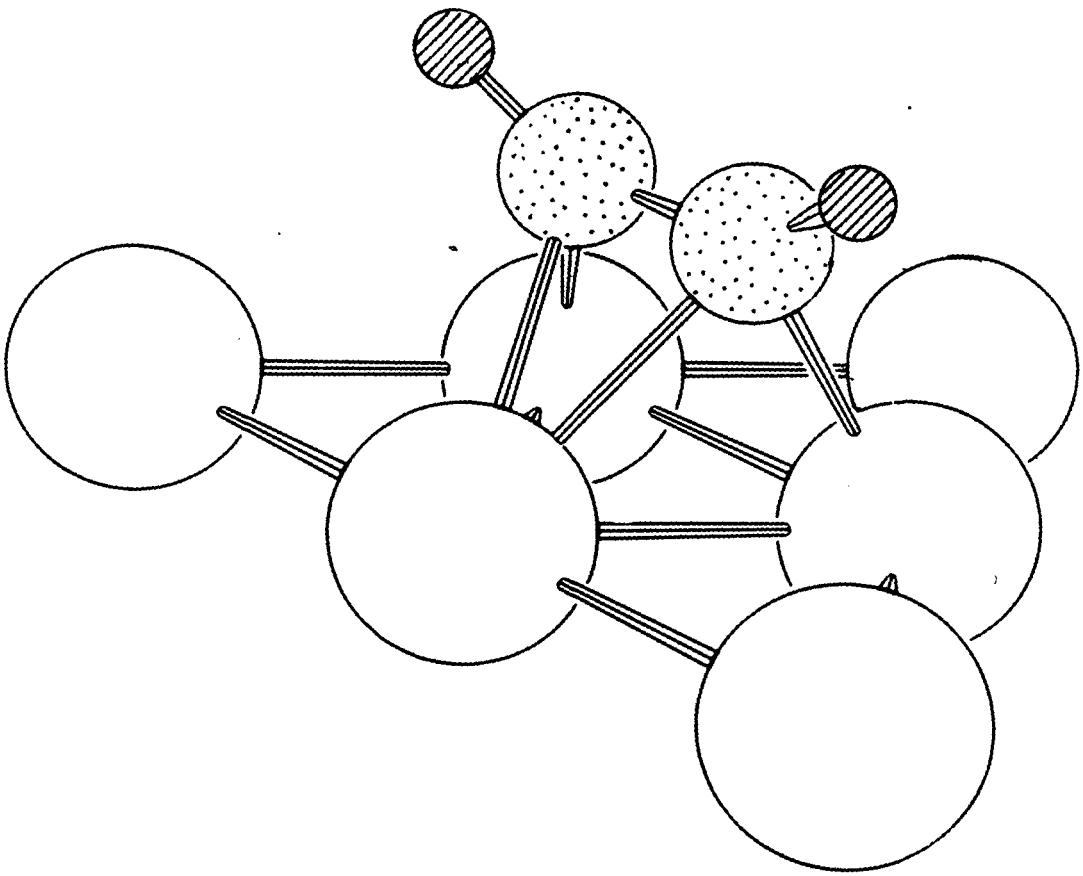

XBL 817-6066

Fig. 16

Substrate	(Gas Phase)	Pd(111)	Rh(111)		Pt(111)
Surface Structure		(3x3)-C_6H_6 + 2CO	(3x3)-C_6H_6 + 2CO	c(2$\sqrt{3}$x4)rect-C_6H_6 + CO	(2$\sqrt{3}$x4)rect-2C_6H_6 +4CO
The Structure of Benzene	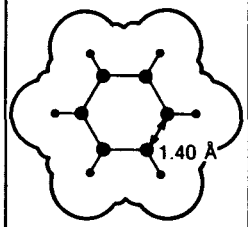	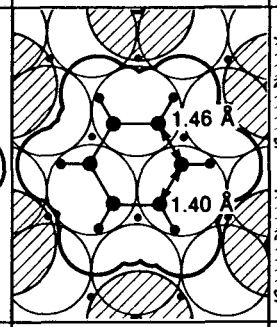	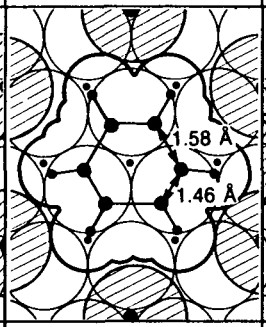	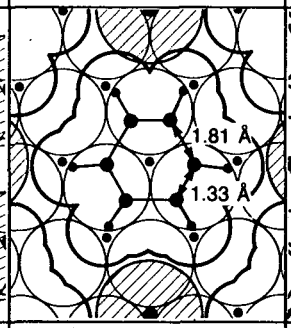	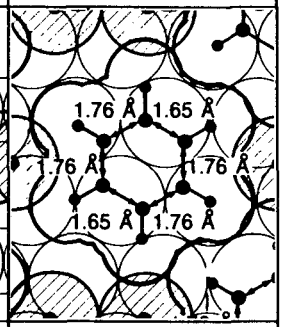
C_6 Ring Radius (Å)	1.40	1.43±0.10	1.51±0.15	1.65±0.15	1.72±0.15
d_{M-C}(Å)	-	2.39±0.05	2.30±0.05	2.35±0.05	2.25±0.05
$\gamma_{CH}(cm^{-1})^*$	670	720-770	780-810		830-850

XBL 878-3565

Fig. 17

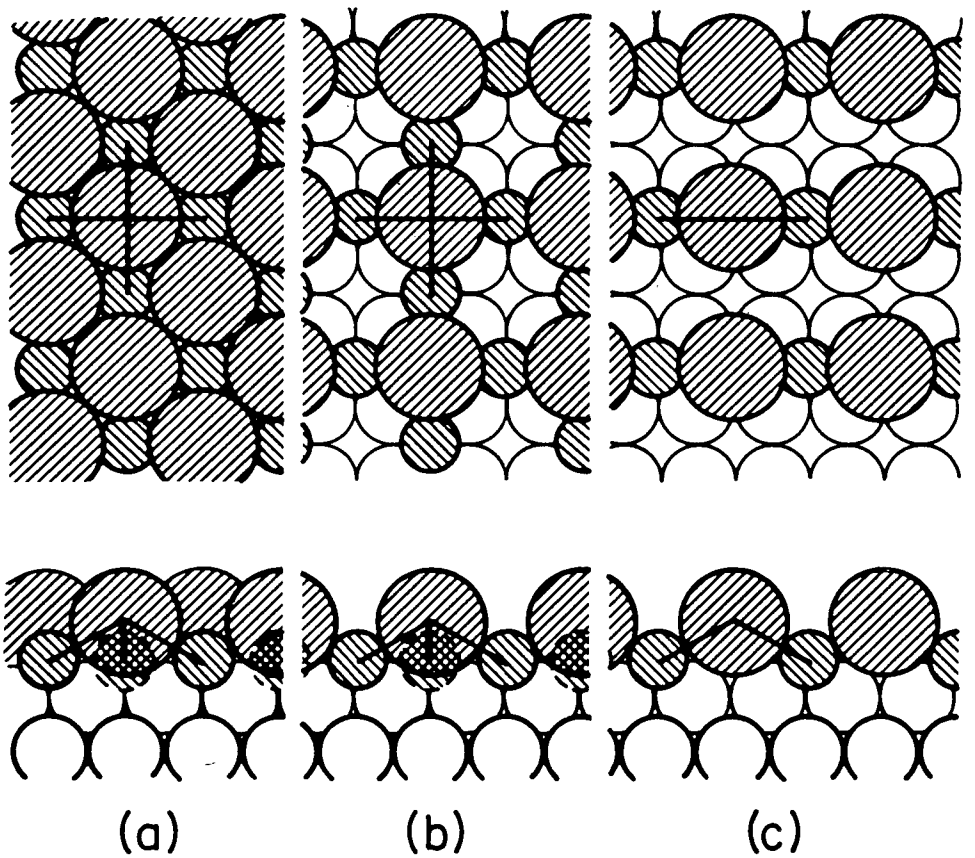

XBL 791-7762

Fig. 18

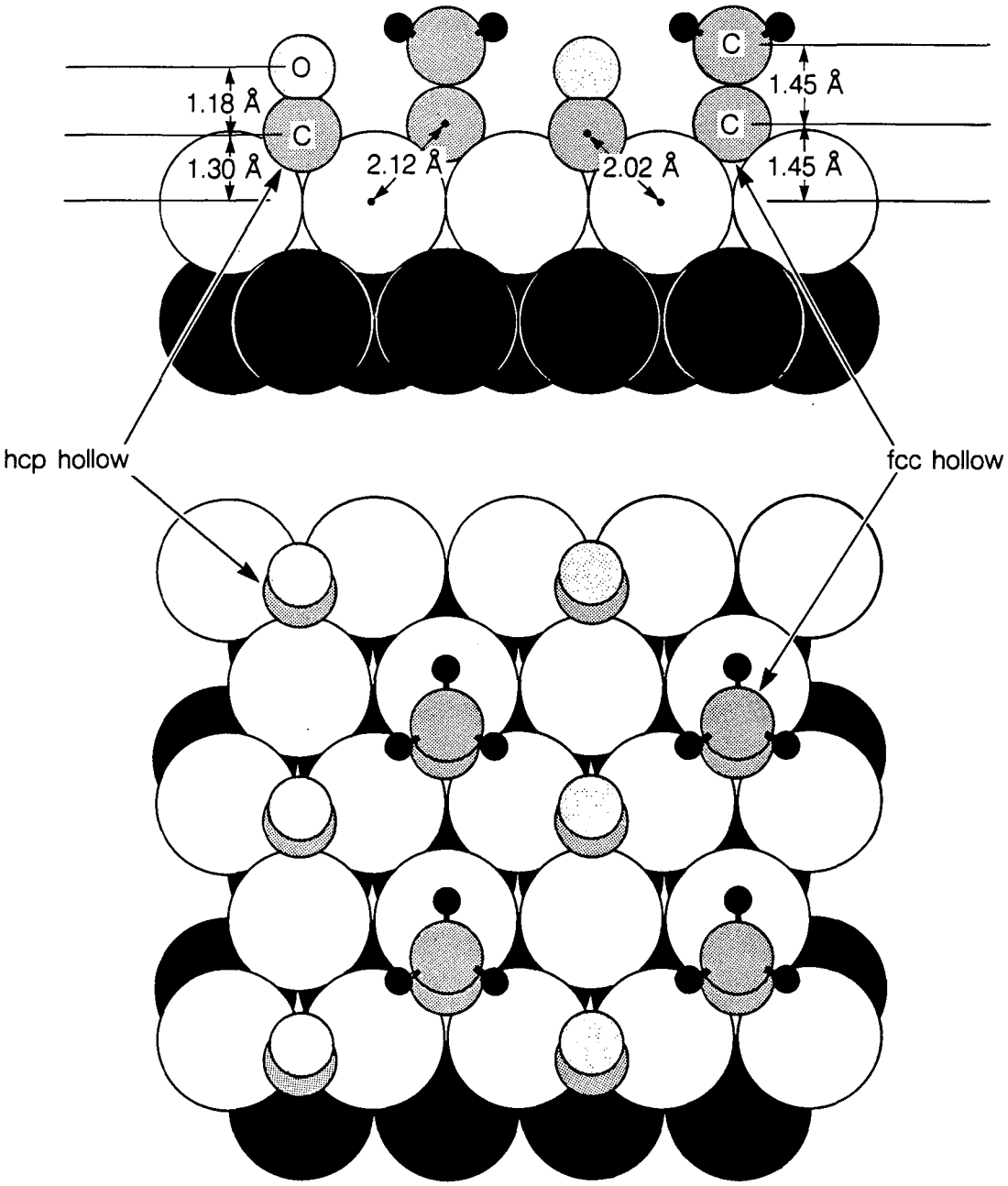

Rh(111) + c(4×2) CO + Ethylidyne(CCH_3)

XBL 877-7004

Fig. 19

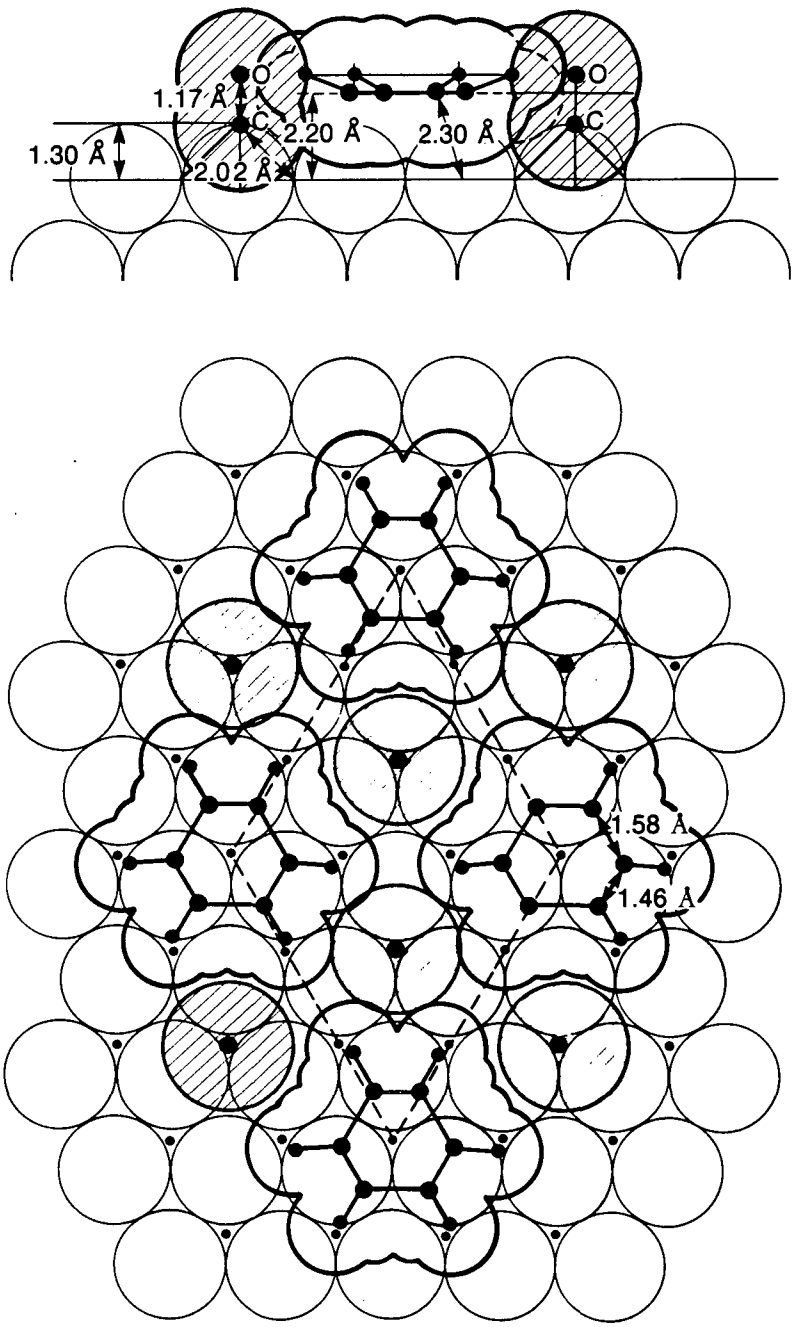

Rh(111) – (3×3) – C_6H_6 + 2CO

XBL 863-10701

Fig. 20

LAWRENCE BERKELEY LABORATORY
CENTER FOR ADVANCED MATERIALS
1 CYCLOTRON ROAD
BERKELEY, CALIFORNIA 94720